5-2016

Diffusion Modeling and Device Development for Peritoneal Membrane Oxygenation

Liana Hatoum

University of Nebraska - Lincoln, liana.hatoum@hotmail.com

DIFFUSION MODELING AND DEVICE DEVELOPMENT FOR PERITONEAL MEMBRANE OXYGENATION

by

Liana Hatoum

A THESIS

Presented to the Faculty of

The Graduate College at the University of Nebraska

In Partial Fulfillment of Requirements

For the Degree of Master of Science

Major: Mechanical Engineering and Applied Mechanics

Under the Supervision of Professor Benjamin S. Terry

Lincoln, Nebraska

May, 2016

DIFFUSION MODELING AND DEVICE DEVELOPMENT FOR
PERITONEAL MEMBRANE OXYGENATION

Liana Hatoum, M. S.

University of Nebraska, 2016

Adviser: Benjamin Terry

Acute respiratory distress syndrome (ARDS) is a pulmonary disease that causes hypoxemia and respiratory failure. The mortality rate for ARDS ranges between 27% and 45%. Current treatments including mechanical ventilation and extracorporeal membrane oxygenation (ECMO) are often associated with high risk complications including barotrauma, infection, thrombosis, and hemorrhage. Alternative pulmonary support techniques are needed to improve the survival rate of patients suffering from ARDS. Previous studies introducing pure O_2 gas, perfluorocarbons and red blood cells into the intraperitoneal (IP) cavity have reported no effect or only a mild increase in oxygenation. Here we report peritoneal membrane oxygenation (PMO) using phospholipid-coated oxygen microbubbles (OMBs). OMBs are oxygen carriers that have unique physical and chemical properties. We hypothesize that IP infusion of OMBs can provide supplementary oxygenation for rats with ARDS and hypoxemia, thus allowing time for essential recovery of the lungs.

We designed a bolus delivery device that automatically and periodically infuses OMBs to the rat's IP cavity. In addition, the device flushes the cavity with saline, scavenges the perfusate, maintains safe intra-abdominal pressure, and regulates perfusate temperatures to body temperature.

In order to understand the mechanism by which intraperitoneal OMB infusion improves systemic oxygenation, we examined, both in theory and *in vivo*, the kinetics of

oxygen transport from OMBs to blood capillaries of healthy rats. A 1D mathematical model was developed using Fick's laws to predict the oxygen diffusion rate across the peritoneum. *In vivo* measurements of the gas content of OMBs after 20 minutes of dwell time in the IP cavity of rats were further used to determine the oxygen diffusion rate, which was found to be within the predicted range. Also, we are able to demonstrate *in vivo* that OMBs not only can provide O_2 to the body, but also can absorb CO_2 and possibly other gases, such as N_2, from the body. PMO represents an alternative extrapulmonary technique of oxygenation and ventilation that is a potential treatment for acute respiratory failure in the future.

Acknowledgements

A special thanks to my adviser and committee chairman Dr. Benjamin Terry for giving me the opportunity to become a research assistant in his lab and for his guidance, leadership, and timely advice over the course of the study. I learned and gained valuable experience in his lab.

I wish to thank the rest of my thesis committee, Dr. Keely Buesing and Dr. Angela Pannier, who were more than generous with their expertise and precious time. Thank you for agreeing to serve on my thesis committee and for your assistance and insightful comments.

I am very grateful for Dr. Jeffrey Shield and Dr. Mehrdad Negahban for giving me the opportunity of becoming a teaching assistant in the first semester of my master's degree. I also wish to thank Kathie Hiatt and Mary Ramsier for their administrative support throughout these years.

I would like to express my gratefulness to PhD student, Nathan Legband, for his great help and for assisting me throughout the study and all of the lab members for their positive feedback.

In addition, I wish to thank Dr. Mark Borden and PhD student, Alec Thomas, from the University of Colorado-Boulder for their collaboration and for fabricating the oxygen microbubbles used in this study. I would like to acknowledge Dr. Douglas Hostetler and Craig Kreikemeier-Bower who helped us in performing the animal

surgeries. In addition, thanks to UNL's Institutional Animal Care staff in housing and caring for the animals used in this study.

Last but not least, my deepest thanks to my husband Hadi for his continuous motivation and support. He was of great help with editing this thesis and other published papers. This work is dedicated to my wonderful parents, my sisters, and my late grandmother.

Table of Contents

List of Figures

List of Tables

Chapter 1: Introduction

Acute respiratory failure is a life threatening condition in which the respiratory system fails in one or both of its gas exchange functions, which include oxygenation and CO_2 elimination [1] [2]. Treatment of patients with severe respiratory failure requiring mechanical support is done in an intensive care unit. Acute respiratory distress syndrome (ARDS) is the most severe form of acute lung injury. It is a rapidly progressive disease that leads to low oxygen levels in blood known as hypoxemia. According to a study in 2005, about 190,000 people in the U.S. develop ARDS annually [3]. Many people who develop ARDS do not survive due to its high mortality, which can be as high as 45% [4]. The risk of death increases with age and severity of illness. Of the people who do survive ARDS, some recover to near-normal function while others experience lasting damage to their lungs. In this study we explore a possible way of oxygenation hoping that this technique may be useful to decrease the morbidity and mortality of patients suffering from ARDS in the near future.

1.1 Scope and Organization of Thesis

Chapter one focuses on the background knowledge on ARDS required to understand the motivation behind this study. Chapter two describes the experimental design and results for finding a reliable way to remove oxygen microbubbles (OMBs) from the intraperitoneal (IP) cavity after injection. Chapter three describes the design and development of an automatic oxygen microbubble (OMB) delivery device, which can be

used for testing the effectiveness of peritoneal membrane oxygenation (PMO) as a treatment for ARDS rats. Chapter four includes the modeling work done to predict the kinetics of oxygen diffusion from OMBs to venous blood in peritoneum tissue. Chapter five describes *in vivo* experiments for gas analysis of OMBs after injection to the IP cavity of rats. Chapter five is a discussion of the findings and conclusions.

1.2 Acute Respiratory Distress Syndrome

1.2.1 Pathophysiology of ARDS

The human lungs are a pair of spongy, air-filled respiratory organs located on either side of the thoracic cavity in the chest. At the microscopic level are small air sacs called alveoli (Figure 1.1 a). Between the walls of the alveoli is a thin layer of cells called the interstitium, which contains cells, fibers, and blood vessels that help support the alveoli. The thickness of the alveolar-capillary barrier is 0.65 μm [5]. The total surface area of the alveoli is approximately 75 m^2 in humans, which is similar to the surface area of a tennis court [6]. Oxygen diffuses from the air in the alveoli to the blood in the small capillaries surrounding the alveoli, while CO_2, a waste product of metabolism, diffuses from the blood to the alveoli, where it can be exhaled.

At the microstructure level, ARDS affects the alveoli in the lungs. Direct or indirect lung injury initiates an inflammatory-immune response that activates neutrophils, macrophages, and platelets to the injured sites [7]. Circulating neutrophils adhere to the endothelium of pulmonary capillaries and release chemical mediators resulting in damage to the alveolo-capillary membrane allowing fluid release from the capillary filling the

alveolar space [8]. When protein rich edema fluid accumulates in the alveolar space, this obstructs the lungs from oxygenating the blood thus leading to hypoxemia (Figure 1.1b). In addition, neutrophils pass through the leaky capillaries and produce an inflammatory response in the lung epithelium, resulting in further damage to the lungs and respiratory decompensation [9]. The release of inflammatory mediators from damaged lung tissue triggers a systemic inflammatory immune response causing multi-organ failure, which is the main cause of death in ARDS patients [10].
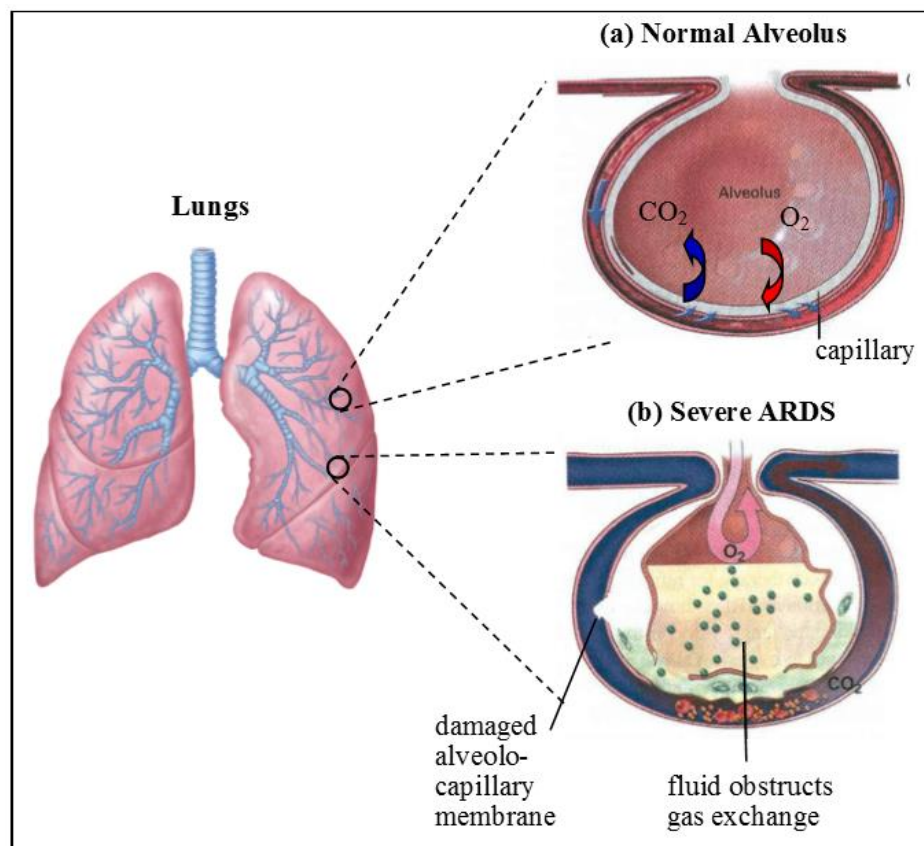
Figure 1.1 Lung alveoli (a) normal and (b) ARDS

Radiographically, a chest X-ray shows bilateral diffuse infiltrates occupying most of the lung fields indicating ARDS (Figure 1.2b). A normal chest X-ray shows clear lung fields (Figure 1.2a).
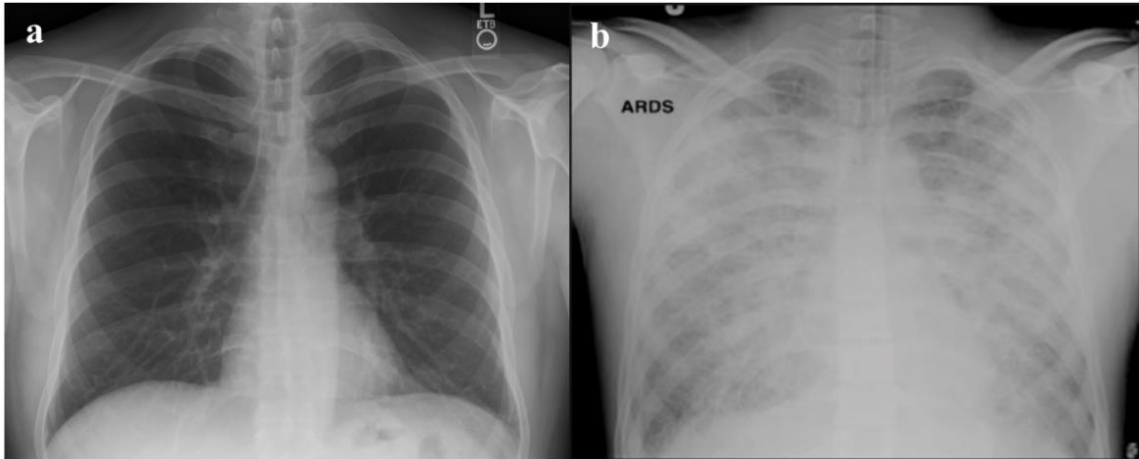
Figure 1.2 Chest X-ray (a) normal patient showing clear lung fields and (b) patient with ARDS showing bilateral diffuse infiltrates [11] [12]

There are several causes of ARDS. Infectious etiologies such as sepsis, bacteremia and severe pneumonia are the most prominent. Systemic inflammatory conditions such as severe pancreatitis can also lead to ARDS. Inhalation of toxic chemicals or smoke can cause ARDS by direct injury to the alveoli and capillaries. In addition, traumatic injuries to the head or chest could contribute to the etiology of ARDS.

1.2.2 Available Treatment for ARDS

The first goal in treating ARDS is to improve the levels of oxygen in the blood to prevent organ failure. For mild disease, oxygen may be delivered through a mask that fits tightly over the nose and mouth to provide supplemental oxygenation. Most people with moderate or severe ARDS will need to be intubated and placed on a mechanical ventilator (MV) to either support or completely control the breathing of the patient (Figure 1.3a) [13]. MV pushes air into the lungs and forces some of the fluid out of the air sacs. It is currently the best treatment option available. However, MV does have side effects. Some patients experience alveolar hyperdistention and cyclic closing and reopening of the alveoli during positive pressure ventilation that leads to volutrauma (increased lung volume) and barotrauma (increased lung pressure). These traumatic changes in lung volume and pressure can lead to ventilator associated lung injury (VALI). VALI can then trigger a pulmonary and systemic inflammatory reaction that may lead multiple organ dysfunction and multiple system organ failure [10]. Although the mortality rate of respiratory illnesses decreased over recent years due to the advances in MV, it still remains high [14].

To support patients with severe ARDS who have failed MV or other conventional ventilator rescue techniques, researchers looked into the idea of extrapulmonary ventilation to bypass the damaged lungs and supply oxygen directly to the blood while allowing the lung injury to heal. Extracorporeal membrane oxygenation (ECMO) is an extracorporeal technique of providing respiratory support to patients whose lungs are unable to provide an adequate amount of gas exchange to sustain life [15]. This method

pumps blood out from the body into a diffusion membrane, artificially adding oxygen into the red blood cells (RBCs) and removing CO_2, and then pumps blood back to the patient (Figure 1.3b). ECMO was first introduced in the 1970's [16]. Historically, ECMO use has centered on neonatal care [17]. A recent increase in adult ECMO use can be attributed to H1N1-induced ARDS across the globe. It is commonly used as a last resort treatment in patients suffering from very severe ARDS. The survival rate of ECMO is 47.7% [18]. ECMO is an invasive technique that has a high cost and complexity, which restrict its use in ambulatory situations. In addition, it is associated with high risk complications such as infection, thrombosis and hemorrhaging [19]. ECMO can support gas exchange in patients failing conventional mechanical ventilation, but proper patient selection and ultimate poor outcomes makes its use controversial. Therefore, alternative pulmonary support techniques are needed to improve the survival of patients with ARDS.
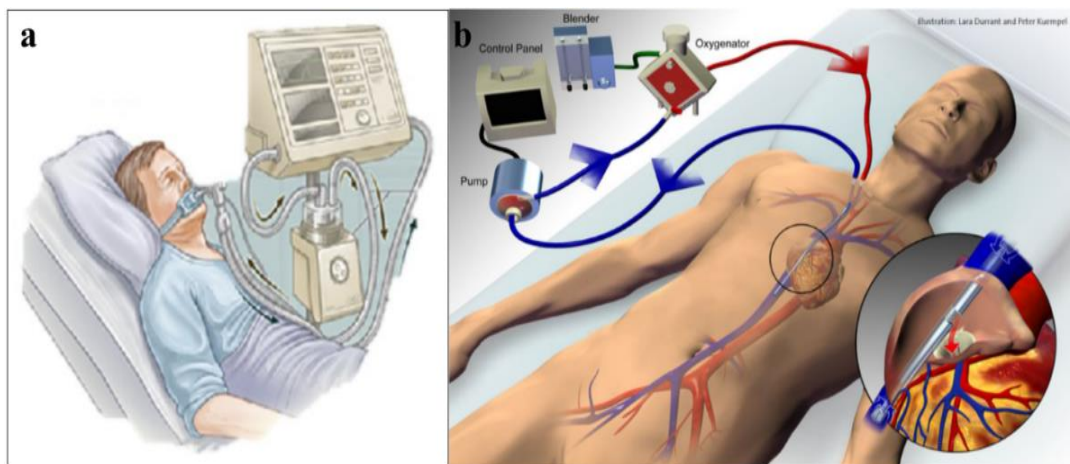
Figure 1.3 Available treatment for ARDS patients. (a) Mechanical ventilation and (b) ECMO

1.2.3 Classification and Prognosis of ARDS

In 2011 a panel of experts established the Berlin criteria to classify ARDS (Table 1.1). ARDS was best classified as mild, moderate and severe based on the ratio of partial pressure of arterial oxygen and fraction of inspired oxygen (PaO_2/FiO_2) [20]. This classification was also based on prognostic measures. As shown in the table below, the mortality rate and duration of mechanical ventilation is proportional to the severity of ARDS and PaO_2/FiO_2 ratio. Patients with severe disease having the highest oxygen need have a high mortality up to 45% and spend on average 9 days on the ventilator, while patients with mild disease have a lower mortality of 27% and spend an average of 5 days on the ventilator.

Table 1.1 Berlin criteria for defining ARDS [20]

ARDS	PaO_2/FiO_2	Mortality (95% CI)	Duration on Mechanical Ventilation (days)
Mild	≤ 300	27% (24-30)	5
Moderate	≤ 200	32% (29-34)	7
Severe	≤ 100	45% (42-48)	9

1.3 Peritoneal Membrane Oxygenation

Alternative extrapulmonary respiration methods have been explored, such as peritoneal membrane oxygenation (PMO). This idea was first proposed in 1934 to mechanically ventilate the peritoneal cavity with oxygen [21]. This idea translates from

the concept of peritoneal dialysis. Peritoneal dialysis is a well-known technique that has

been widely accepted for the treatment of end stage renal failure since 1923 [22]. This

technique exchanges solute and fluid across the peritoneum and is simple and less

expensive than hemodialysis (Figure 1.4) [23]. The most common complications from

peritoneal dialysis include infection around the catheter site or infection of the lining of

the abdominal wall also known as peritonitis.
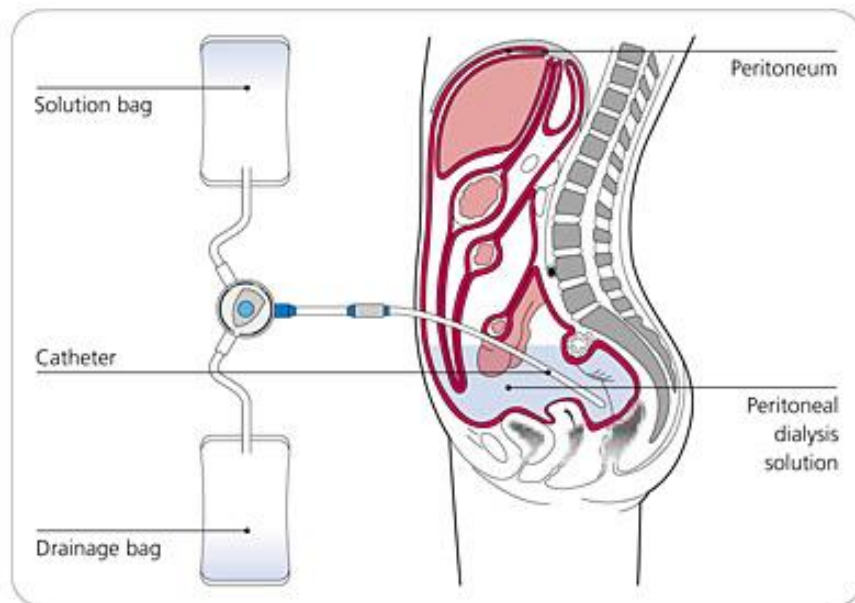
Figure 1.4 Peritoneal dialysis [24]

The peritoneum is a thin, continuous, translucent membrane, which covers the

visceral organs and the abdominal wall. It is composed of a mesothelial single cell layer,

interstitial tissue and blood capillaries. The average surface area of the peritoneum

membrane (PM) is 1.3 m^2 in adults [25]. PMO follows the same concept as dialysis, but

uses the peritoneum for gas exchange. This method shows promise as it is a simple

procedure with easy access of the peritoneal cavity for catheterization, and relative safety with low risk complications compared to an extracorporeal circuit [26] [27].

One study observed the effects of transperitoneal ventilation with pure O_2 gas on death time in asphyxiated rabbits [28]. All animals died successively after asphyxia. In addition, there was no significant increase in PaO_2. This study failed because the surface area was minimized owing to the high surface free energy (~73 mJ/m^2) of the gas/water interface. Another study aimed to determine whether systemic oxygenation could be increased in pigs, with induced hypoxia, by perfusing the abdominal cavity with oxygenated perfluorocarbons (PFCs) [29]. The most clinically relevant results occurred at an FiO_2 of 14%, resulting in a baseline mean PaO_2 of 39.4 ± 5.0 mm Hg with oxygenated saline solution perfusion, and a mean PaO_2 of 55.3 ± 7.6 mm Hg with oxygenated PFC perfusion. Infusion of RBCs into the intraperitoneal (IP) cavity of dogs resulted only a mild increase in oxygen partial pressures [30]. These prior attempts have not been able to show clinically relevant results. This may be due to the low biocompatibility and low oxygen transfer efficiencies of the oxygen carrier utilized, which might explain their failure to oxygenate the body. The most successful application of peritoneal oxygenation used liposomal synthetic hemoglobin, which produced a mean increase in rat cardiac arrest time following a right pneumothorax from 9 to 33 min [31].

Our proposed solution is to us oxygen microbubbles (OMBs), an innovative oxygen carrier with unique physical and chemical properties. The original clinical utilities of gas-filled particles are as ultrasound contrast agents filled with an inert insoluble gas and drug delivery vehicles [32]. Such suspensions are not well suited for

gas delivery because they are typically designed to have low gas fractions and prolonged circulation. However, OMBs (70% vol) are designed to be smaller than 15 μm in diameter suspended in saline (30% vol). They contain pure O_2 gas core encapsulated by a phospholipid monolayer composed of 1,2-distearoyl-sn-glycero-3-phosphocholine (DSPC) and polyethylene glycol (PEG) brush combined in a 9:1 molar ratio (Figure 1.5). PEG forms coils (~10 nm in height) that provide steric repulsion to prevent microbubble coalescence. The phospholipid monolayer membrane is 3 nm thick, which reduces surface tension and provides rigidity. The bubble's shell comprises only ~1% of the total microbubble volume. OMBs mimic the structure and composition of natural lung alveoli. The bubble shell is highly permeable to O_2 and other gases, allowing continuous diffusive exchange with surrounding dissolved gases [33].
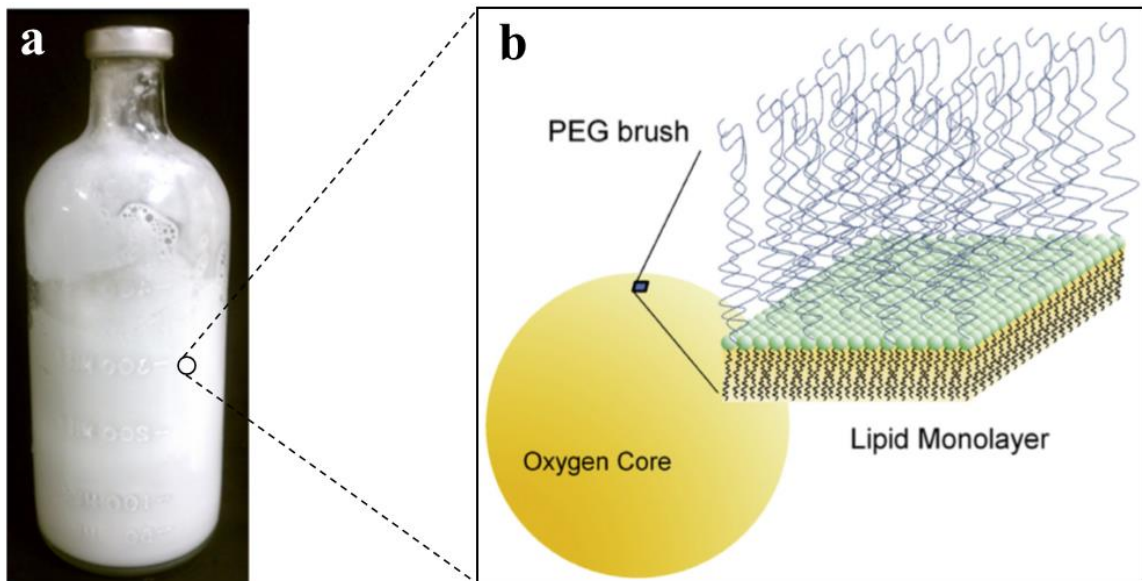
Figure 1.5 (a) OMB vial and (b) microstructure of OMBs [34]

A 70% volume suspension of OMBs at atmospheric pressure and 37 °C contains an estimated 0.88 mg-O_2/mL [34]. Table 1.2 compares the oxygen carrying capacity of RBCs, PFCs, liposomal hemoglobin (Hb), and pure oxygen gas. OMBs can carry oxygen 0.88 mg-O_2/mL, which is higher than other aqueous carriers used at same temperature and pressure. Although pure O_2 gas has 1.26 mg-O_2/mL, the oxygen carrying capacity is not the only criterion for efficient oxygen transport. Oxygen diffusion also depends on the surface area by Fick's law relation. The overall rate of diffusion of gas is equal to the product of the flux and area. Pure oxygen gas in the peritoneal cavity has a high surface free energy (~73 mJ/m^2) of the gas/water interface. Thus, the surface area for diffusion is drastically minimized [34].

Table 1.2 Oxygen carrying capacity at body temperature and atmospheric pressure

O_2 carrier	OMBs	RBCs	Liposomal Hb	PFC	O_2 gas
Capacity (mg-O_2/mL)	0.88	0.31	0.62	0.57	1.26

A recent study by Kheir et al. [35] characterized the release kinetics of O_2 gas from OMBs to blood. When OMBs were mixed with human deoxygenated blood *ex vivo*, O_2 diffusion was complete within only 4 sec. They also investigated intravenous injection of OMBs in rabbit hypoxic ventilation and tracheal clamp asphyxiation. OMBs supplied the animals' full oxygen consumption for 15 min, and decreased the incidence of cardiac arrest and organ injury from asphyxia. The intravenous treatment with OMBs appears to be a promising method for short-term rescue. However, prolonged continuous infusion of

OMBs into the bloodstream has risks of embolism, thrombosis, and toxicities of lipid and saline that remains in blood circulation. Therefore, a different approach is needed for long term therapy of ARDS avoiding complications associated with injection of OMBs into the bloodstream.

Previous work has shown that OMBs delivered intraperitoneally maintain hemoglobin oxygen saturations at normal levels and provide 100% survival for rats with a right-sided pneumothorax for at least 2 hours. In comparison, untreated rats and rats treated with peritoneal oxygenated saline died within 30 min [34]. Another study showed that PMO therapy can double the survival time of rabbits after complete tracheal occlusion from 6.6 ± 0.6 min (average $\pm$ SD) for the saline controls to 12.2 ± 3.0 min for the bolus OMB treated rabbits [36]. These results show that OMBs have potential to be an alternative mechanism of oxygen delivery when injected intraperitoneally.

Previous work characterized the properties of OMBs *ex vivo* [37] [33], but there is a need to conduct research to study the rate of oxygen delivery *in vivo*. Also further studies are needed to test the potential of OMBs in absorbing CO_2 *in vivo*. Our team recently demonstrated that PMO can significantly increase survival in rats suffering a right pneumothorax and rabbits suffering complete tracheal occlusion. In order to proceed into a more clinically relevant disease model, the goal of the proposed study is to develop and test PMO therapy in a clinically relevant rat model of mild to severe ARDS in rats. We hypothesize that intraperitoneal infusion of OMBs can be used as a supplementary method of oxygen delivery and CO_2 removal for rats with ARDS thus allows time for essential recovery of the lungs.

1.4 Research Objectives

The overall goal of this research is to considerably increase the survivability of patients with ARDS by providing alternative extrapulmonary oxygenation using OMBs. In pursuit of this goal, the specific aims of this research is to first finalize the development and validation of an OMB delivery system that will automatically infuse and remove OMBs from the rat's IP cavity. This device can be used for a long term study for testing PMO as a potential treatment for ARDS in rats.

We aim to understand the mechanism by which intraperitoneal OMB infusion improves systemic oxygenation, by examining the OMB gas exchange properties with the PM by both theoretical modeling and *in vivo* tests. A one dimensional mathematical model developed using Fick's laws can predict the oxygen transport rate from OMBs to peritoneum blood. A model would help us understand in theory the kinetics of oxygen transport and how that would relate to the normal oxygen consumption need in rats. In addition, it can predict whether continuous infusion or periodic bolus infusion of OMBs is more efficient in oxygen delivery. One way for experimental validation of the model is by measuring O_2 delivery and CO_2 removal by OMBs after infusion to the IP cavity of rats. These measurements can be used to calculate the oxygen diffusion rate *in vivo* and compared to our modeled oxygen kinetics. Finally, we aim to determine the optimal perfusion dosage and dwell time of OMBs in the IP cavity of rats.

Chapter 2: Aspiration of OMBs from the Intraperitoneal Space

2.1 Introduction

Injection of OMBs into the IP cavity of rats can be applied by a needle or a catheter implanted in the lower abdomen. The purpose of this experiment is to find a reliable aspiration technique of OMBs after an IP injection. Aspiration is needed in experiments involving studying the gas content of OMBs after dwelling in the IP space. In addition, IP infusion of OMBs for several days to treat ARDS will lead to accumulation of saline and lipids in the IP cavity. If intra-abdominal pressure exceeds safe limits this could interfere with the hemodynamics of the abdomen and limit the blood supply to abdominal organs. In order to prevent inducing abdominal compartment syndrome, OMBs need to be removed from the IP space. Previous attempts by our group to aspire the injected OMBs after dwelling in rat's IP cavity were unsuccessful using small needles. In this experiment, different needle diameters were tested, in addition to a side opening teat tube (SOTT), and a peritoneal lavage catheter (PLC) (Figure 2.1a,b).

2.2 Materials and Methods

Male Wistar rats ($n = 5$, m = 539 g) were housed and acclimated for four days, and cared for according to the University of Nebraska-Lincoln Institutional and Animal Care and Use Committee (IACUC) guidelines. All rats were sedated using ketamine-

xylazine (18-2 mg/kg) and placed in the supine position on a warming pad (T/pump Classic, Gaymar) set at 38 °C to maintain body temperature. Paw pinches were made to verify full sedation. The rat was then placed in a supine position on the surgery table.

Previous studies showed that an IP volume injection of 60 mL was considered to be safe for ~ 500 g rats [38] [39]. OMBs were stored in a cooled environment at 5 °C prior to the experiment to preserve their composition and structure. A 60 mL syringe was used to extract OMBs from the vial, and the syringe was left at room temperature for 5 minutes. A 60 mL single bolus of OMBs was injected into the IP cavity within 1 minute. After injection, OMBs were allowed to dwell for 2 minutes so that OMBs were naturally distributed inside the cavity. After dwell, OMBs were manually aspirated by pulling out the plunger of the syringe. The volume of OMBs aspirated was recorded, and the aspirated OMBs were transferred into a waste beaker. The same volume of fresh OMBs was injected in the IP cavity using the next larger needle and allowed to dwell for 2 minutes. This preserves a total of 60 mL OMBs in the IP cavity. Three different methods were tested, which include needles of increasing size (18G, 16G, 14G, 11G, and 10G), an SOTT, and a PLC (JP7, Mila International, Erlanger, KY) catheter were tested. Table 2.1 shows the inner diameter (ID) and length of the needles, SOTT, and PLC used. For the 11G, 10G, and SOTT, a scalpel was used to make a small incision in the lower right quadrant of the abdominal cavity to accommodate for the larger diameters. All items were placed in the same incision to minimize injury to the rat. For placing the catheter, a small incision into the skin was made to expose the fascia of the abdominal wall. A PLC

outflow catheter (PLC) was surgically implanted in the IP cavity and sutured to the skin.

Finally, the rat was sacrificed using CO_2 inhalation.

2.3 Statistical Analysis

Multiple t-tests assuming equal variances was performed on the volumes of aspirated OMBs to test for any differences between all groups. All tests used the same level of significance ($\alpha = 0.05$).
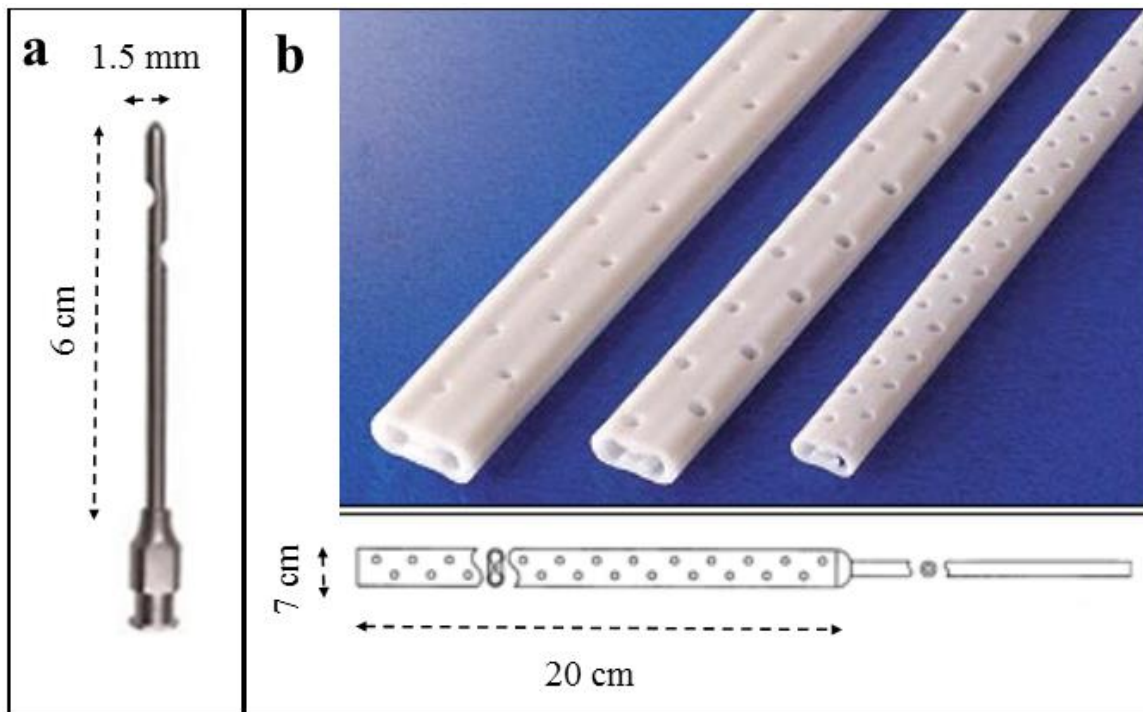
Figure 2.1 Items tested for aspirating OMBs (a) Side opening teat tube and (b) peritoneal lavage catheter

Table 2.1 Size of the needles and catheters tested for aspiration of OMBs

Size	Needles					Cannula	Catheter
	18G	16G	14G	11G	10G	SOTT	PLC
ID (mm)	0.8	1.2	1.6	2.4	2.7	1.5	7
Length (cm)	2	3.8	2.5	2	2	6	20

2.4 Results and Analysis

The aspirated volumes of OMBs are shown in Appendix A. The means $\pm$ SD were plotted on a bar graph in Figure 2.2. The PLC had the highest average of aspired volume of 30 ± 6.3 mL. There is significant statistical difference between the means of PLC and each of SOTT, 10G, 14G, and 18G needles ('***' p<0.001).

Volumes of approximately 0 mL OMBs aspirated were due to omental occlusion (OO). Occlusion occurs when fatty abdominal tissue (omentum) occludes the tip of the needle while applying a suction force using the syringe. Table 2.2 summarizes the frequency of OO occurrence for each item. Occurrence of omental occlusion (per 5 rats) was between 2 to 4 using needles (between 18G and 10G) compared to none using the lavage catheter. In other words, during aspiration needles had a high failure rate of $50 - 80\%$, while the PLC had 0% failure.

Table 2.2 Frequency of omental occlusion occurred using each item (n=5)

Item	18G	16G	14G	11G	10G	SOTT	PLC
Frequency of OO	3	2	4	3	3	1	0
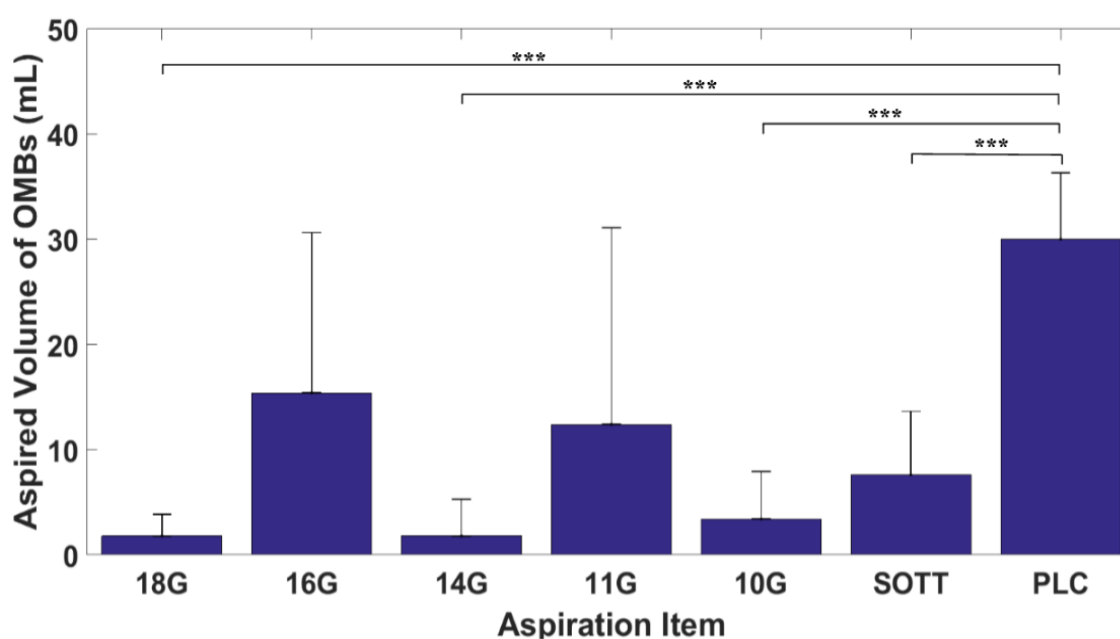
Figure 2.2 Aspiration volumes (mean ± SD) of OMBs using different items. Significant difference is indicated by '***' (p<0.001)

The needles had a wide range of aspiration volumes of spent OMBs ranging from 0 to 43 mL. The variation was mainly due to the high probability of omental plug during aspiration. PLC successfully aspirated an average of half of the injected OMBs, with a relatively low SD over the 5 trials. PLC has proven to be the most reliable and efficient

method to extract the OMBs. Its advantages over needles and SOTT are its flexibility, wider diameter, its numerous pores and increased length that allows a large surface area in the IP cavity and subsequently allows better aspiration of OMBs. Thus, PLC can be used for long term studies were it can be surgically implanted in the IP cavity unlike needles or SOTT. In addition, the PLC can be used in experiments that require extraction of OMBs from the IP space for gas content measurements.

Chapter 3: OMB Infusion Device

3.1 Introduction

The mortality rate of patients with ARDS remains high even with the advancements in mechanical ventilation and ECMO. Alternative extrapulmonary ventilation techniques such as peritoneal membrane oxygenation are still being explored as a potential therapy for ARDS. With the development of a promising oxygen carrier, a device is needed to deliver OMBs intraperitoneally. The system will be used for studying PMO with conscious and ambulatory rats of mild to severe ARDS. To evaluate improvements of oxygen levels in blood and survivability, the length of the study will be at least 3 days after inducing ARDS to rats and administering OMB treatment. Manual infusion and removal of the perfusate to the cavity is a time consuming and exhaustive procedure. In addition, continuous or periodic infusion of OMBs for several days results in accumulation of lipids and saline (30% vol) in the IP space thus could limit the blood supply to abdominal organs if IP pressure exceeds safe limits. Therefore, an automatic system for infusion and scavenging of OMBs is needed for this study.

The design of the delivery device was established in a manner similar to peritoneal dialysis catheter placement. A preliminary design was developed for continuous infusion of OMBs, which consisted of two catheters implanted in the cavity, one for inflow, and PLC for outflow. However, *in vivo* testing of the continuous infusion system first prototype revealed advanced tissue obstruction and growth in the PLC after four days. This was a major problem as it prevented further removal of fluid from the

cavity. In addition, OMBs need to dwell in the cavity for gas exchange to occur (Chapters

4 and 5).Therefore, the design was revised to implement a periodic bolus system that is

simpler and effective. This chapter focuses on describing the current bolus delivery

system. The device will automatically infuse and scavenge OMBs, maintain safe intra-

abdominal pressure, and regulate perfusate temperatures to body temperature.

3.2 Materials and Methods

A schematic of the delivery system (Figure 3.1) includes OMB storage, periodic

infusion of OMBs, intra-abdominal pressure (IA) pressure measurement and control,

temperature measurement and control, tubing restraint, data acquisition and LabVIEW

control.
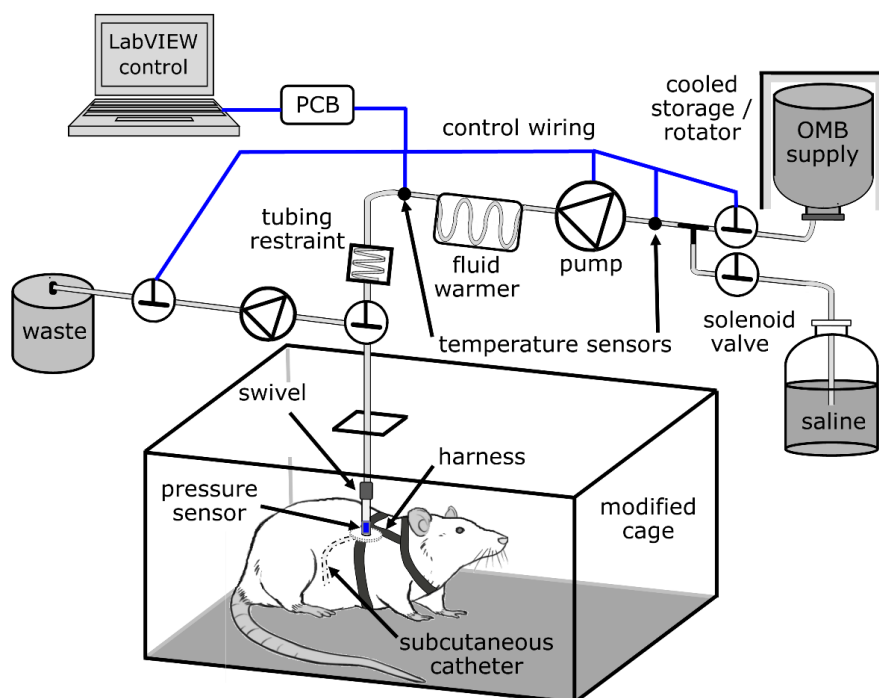
Figure 3.1 Schematic of the bolus delivery system for conscious rats

3.2.1 OMB storage

OMBs require a cool, rotating, and pure humid O_2 environment to avoid breakdown of the lipid monolayer in the bubbles. The OMB vial is stored in a container at a temperature between 2-8 ℃ and placed on a rotating table. The OMB vial is connected to an inlet line for suppling pure O_2 gas, an O_2 outlet line to avoid over pressurizing the vial, and an OMB supply line (Figure 3.2). To avoid evaporation of the saline in OMBs, pure O_2 gas is supplied to a closed vial containing water, which supplies humidified O_2 gas to the OMBs vial.
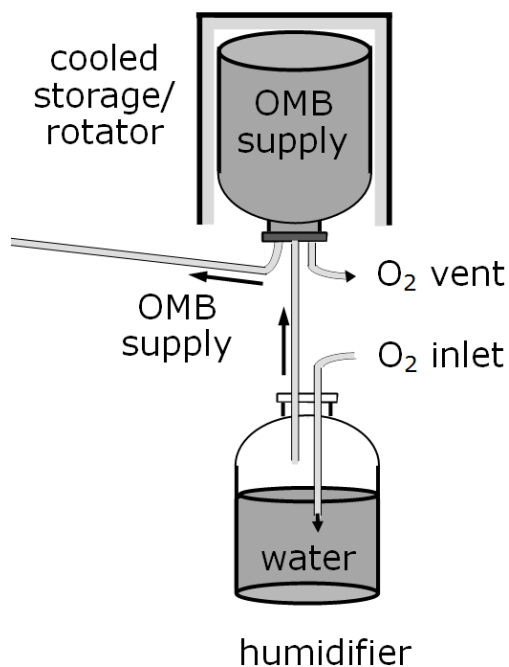
Figure 3.2 Humidifier for OMBs

3.2.2 Infusion

The fluid infusion system necessary to supply OMBs without exposing the infusing fluid to the pump and surrounding atmosphere. The system delivers OMBs by a peristaltic pump (FH100M, Thermo Fisher Scientific, Waltham, MA) shown in Figure 3.3. OMBs pass from the storage vial through tubing, connectors, valves, and swivel before reaching the cavity. This closed loop system avoids air contamination of OMBs to preserve their oxygen content. The system requires only a single peritoneal catheter that is used as both an inflow and outflow line. The PLC is tunneled subcutaneously to the back of the rat where they are fixed to a custom pedestal at least 3 days prior to the beginning of the study. The perfusion circuit includes connecting tubing to the infusion/scavenge ports of the PLC to the pump. The pump has a flow rate range of 0.013-760 mL/min and a maximum output of 200 rpm. This pump has an extended rotor head for multiple tubing lines, which allows the ability to infuse multiple subjects or multiple fluids. The adjustable cartridges allow most tubing diameters to be used for infusing. The pump has a DB-25 input/output with 0-10 V, which allows for it to be controlled using a LabVIEW program.

Figure 3.3 Peristaltic pump used for infusion

3.2.3 Pressure Measurement and Control

In order to prevent over pressurizing the cavity that could limit blood flow to the region and can lead to abdominal compartment syndrome, IA pressure is measured and maintained between $0 - 6$ mmHg [40] [41]. For measuring the IA pressure of rats non-invasively, a pressure transducer (S7d, Gaeltec Devices Ltd, Isle of Skye, UK) is inserted into a catheter for continuously reading pressure throughout the length of the study. The sensor (6 French) is inserted into the inflow/outflow line at a negligible height over the catheter port to avoid inaccuracy in the IA pressure reading.

The S7d is powered by a low voltage mains adaptor 9V DC with sensitivity of 5μV/V/mmHg. For completely accurate pressure measurements, the transducer is compared to a calibrated pressure sensor. The transducer is connected to an amplifier

(S7d pressure transducer amplifier, Gaeltec Devices Ltd), which has an LCD display and is connected to a 4 channel box (Figure 3.4). Also, it has an analog voltage output port that can be connected to a data acquisition system.
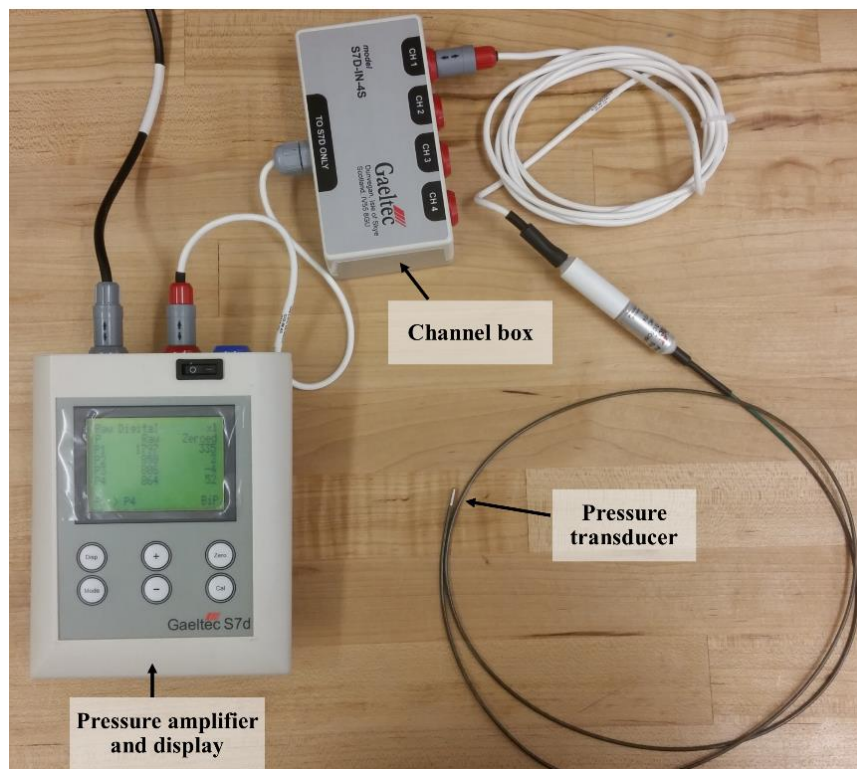
Figure 3.4 Pressure measurement and display

Pressure is regulated through the use of a fluidic control solenoid valve controlled by LabVIEW. In case IA pressure exceeds 6 mmHg, the outflow solenoid valve opens and a scavenge phase is initiated so that OMBs are extracted from the IP cavity until the IA pressure goes back to the safe range.

3.2.4 Temperature Measurement and Control

OMBs are stored at low temperatures to preserve their structure and stability for approximately 7-10 days. Before infusing OMBs in bolus volumes to the rat's IP cavity, they need to be warmed close to body temperature to avoid inducing hypothermia. The fluid warmer (i-Warm, Midmark, Kettering, OH) is a dry-heat device designed for warming I.V. fluids safely through the heating plate (Figure 3.5). Measurements of the temperature of the OMBs both in their storage and after passing through the fluid warmer are needed to verify they are within the required ranges. To measure the temperatures, a K-type thermocouples are used. One sensor is placed in a T connector at the fluid warmer exit line. Another sensor is placed in the OMB storage to verify the temperature is between 2-8 ℃. The thermocouple output is amplified with an AD595-AQ amp (Burr-Brown, Digikey, Thief River Falls, MN). The output of the amplifier is 10 °C/mV. The project circuit board (PCB) is designed on Altium to connect the electronics (Appendix B). The circuit includes two K-type thermocouples, two amplifiers, +5 V power supply, ground, and two voltage outputs. The PCB is then fabricated by the UNL Engineering Electronics Shop (Figure 3.6).

Figure 3.5 Fluid warmer
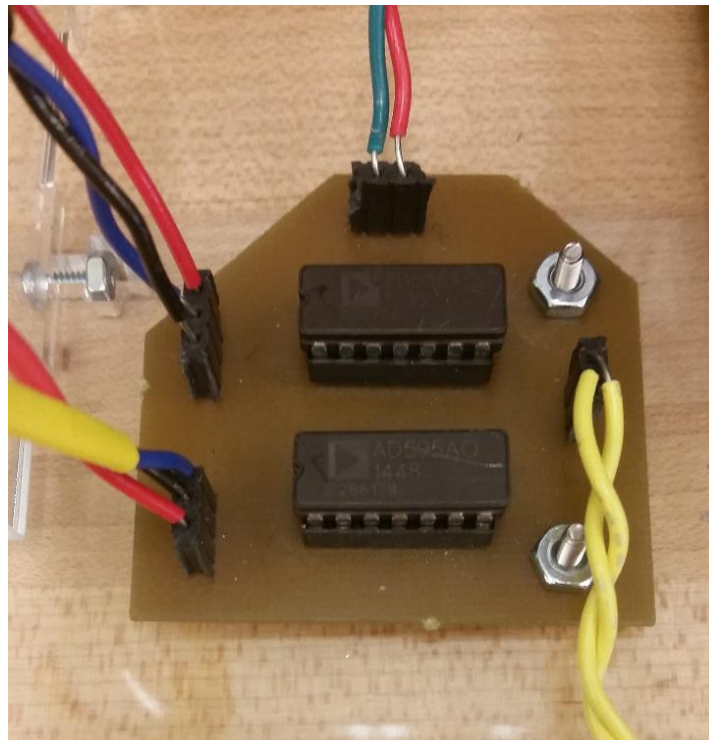
Figure 3.6 PCB for temperature measurement

3.2.5 Tubing restraint

In order to prevent tubing from restraining the rat or being damaged by the rat, a spring restraint is originally designed with a spring retractor and a counter balance weight. Preliminary trials of the first prototype revealed that this tubing restraint did not work properly. One rat managed to reach the tubing and pull on his catheter. Therefore, a new design for a rat tether is under development.

The tubing will be tethered to the infusion pump via a custom swing arm that keeps the tubing suspended above the rat and prevents entanglement (Figure 3.7). Once in the cage, the animal will have free access to food and water.

Tethered systems require an in-dwelling catheter, a harness, and swivel. Tethered infusion is a commonly employed technique in laboratory animals, especially rats. This is the only option for long-term continuous access in rats [42]. The rat harness serve to protect the catheter port and with minimal stress, a means of restraining the animal.

In addition, a counterbalance serves to reduce the weight load that the animal experiences from the tether and swivel. An important component between the rat and the pump is the swivel, which serves as a rotary fluid seal. Without the swivel, the animal would be significantly encumbered in its movement, and the fluid line would occlude partially or totally.
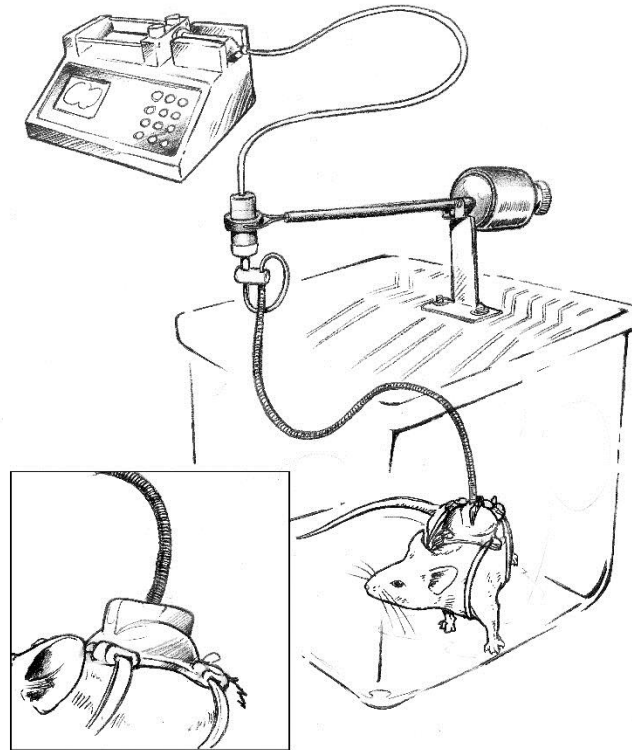
Figure 3.7 Rat tether [42]

3.2.6 Data Acquisition

To connect the peristaltic pump to the DAQ (USB-6003, National Instruments, Austin, TX), a DB-25 break out board (Winford Engineering, Auburn, MI) is required. Figure 3.8 shows the electronics box that includes 4 solid state relays, a breakout board, DAQ, and temperature PCB. The acrylic box design using SolidWorks is shown in Appendix C.
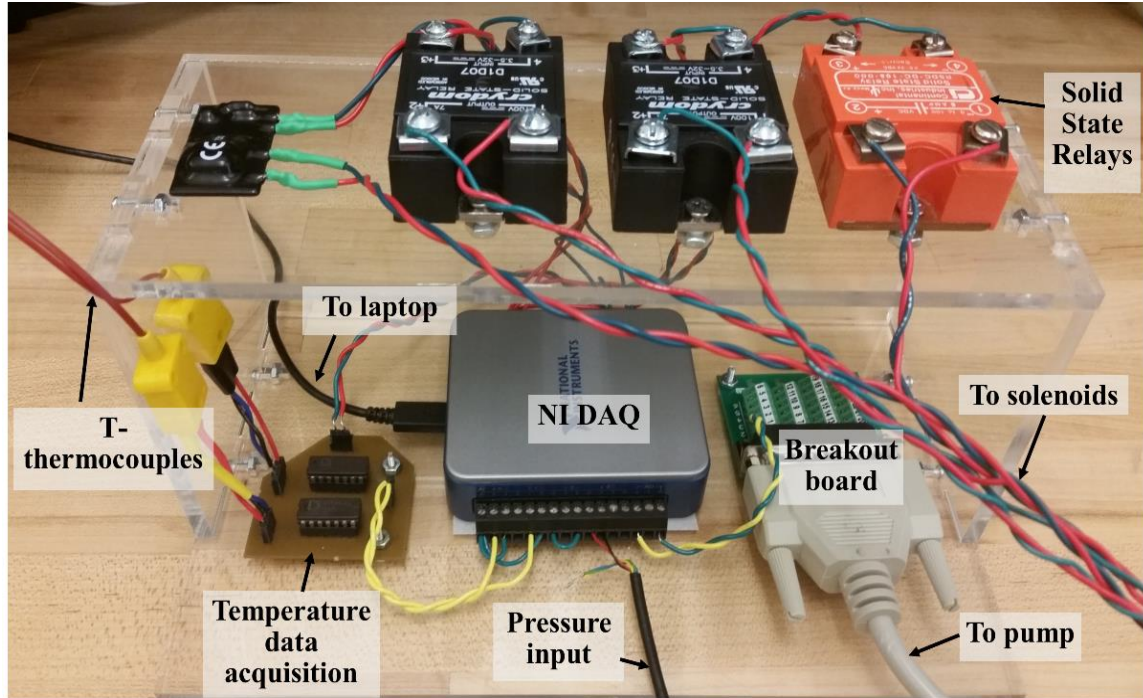
Figure 3.8 Electronics box

3.2.7 LabVIEW Control

The delivery device includes a LabVIEW interface shown in Figure 3.9 to control several key parameters such as rat's mass, pump speed, and type of infusate, which is either saline or OMBs. In addition, the program provides manual override that allows the user to control the pump and the four solenoid valves or stop the system completely. The control program automatically calculates the bolus volume (BV) based on the rat's mass (M) as: BV (mL) = M (g) /10

Figure 3.9 LabVIEW control user interface

3.2.8 Testing the System

For preliminary trials to test the continuous system, male Wistar rats (n = 2, m ~ 500 g) were successfully administered aerosolized (Lipopolysaccharide) LPS endotoxin to induce ARDS. One rat was continuously infused OMBs at 0.5 mL/min for 12 hours and the other for 24 hours. Another trial was conducted on a rat for 4 days for testing the automatic infusion and scavenging system. Benchtop tests were conducted on the final design of the automatic bolus system.

3.3 Results and Analysis

In ARDS rats, S_pO_2 decreased steadily following administration of endotoxin in untreated controls while S_pO_2 increased after 24 hours for ARDS rats treated with OMBs

(Figure 3.10). The device lacked automatic scavenging with a waste flow line. Instead, excess OMBs were removed by manually drawing them out from the cavity with a syringe connected to the PLC every 2 hours.

One preliminary trial on a rat was conducted with the automatic continuous infusion and scavenging system and it revealed that there was advanced tissue obstruction and growth in the PLC after four days. This may be caused by the constant suction applied to the outflow line leading to suction of tissue inside the pores of the lavage catheter.

Benchtop testing of the final design of the bolus delivery system has been successfully completed. The tubing restraint was not working properly. The new design of the rat tether is still under development. The bolus delivery system will be tested on rats to ensure that infusion and scavenging can be maintained for two weeks. Once testing is successful, we will proceed with validation trials with saline, inert gas microbubbles, and OMBs.
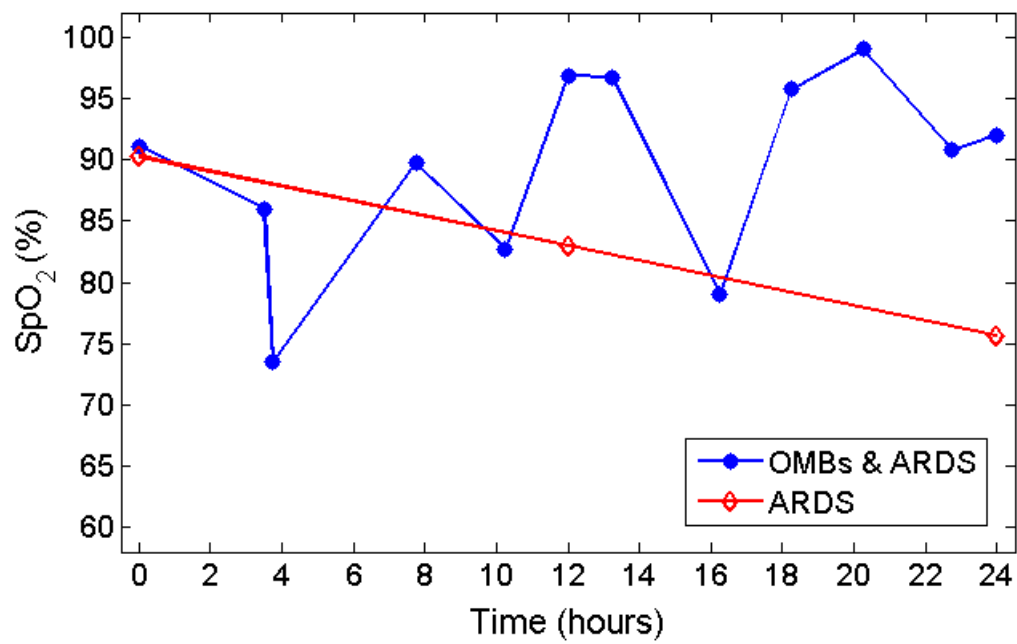
Figure 3.10 Oxygen saturation taken by pulse oximetry [43]

Chapter 4: Diffusion Modeling

4.1 Introduction

A previous theoretical and experimental study was undertaken by Borden et al. to determine the fate of a microbubble suddenly suspended in a multi-gas environment, such as the bloodstream [33]. They developed a numerical model based on the classic Epstein and Plesset theory that predicts the rate of microbubble dissolution in a single gas medium. Experimental verification of the model was performed with individual sulfur hexafluoride (SF_6) microbubbles coated with a soluble surfactant. Microbubbles placed in a perfusion chamber containing N_2 and O_2 in an aqueous medium initially grew due to the influx of nitrogen and oxygen and then dissolved under surface tension.

In contrast, our study involves infusion of oxygen filled microbubbles into the intraperitoneal cavity of rats with ARDS. This is a new method being explored that requires more studies in theory and *in vivo*. A lack of literature on modeling oxygen delivery from OMBs to peritoneum tissue prompted a need for this study. In addition, there is not enough data that support one method of infusion in delivering oxygen (bolus vs. continuous circulation). A model for diffusion would predict how fast oxygen diffuses across the multiple layers of tissue in the surrounding abdomen. Depending on how fast diffusion reaches steady state, this would determine the maximum dwell duration of OMBs. A simple 1D mathematical model was developed using Fick's laws to determine the oxygen transport rate and how it compares to the normal oxygen consumption need.

4.2 Materials and Methods

For OMBs injected into the IP cavity of rats, the pathway of gas exchange across the PM is assumed to be homogeneous and has one spatial dimension for simplification. OMBs are assumed to have a constant O_2 concentration when injected in the IP cavity and no oxygen is consumed by surrounding tissue. The gas components are assumed to behave ideally and no convection occurs.

Oxygen molecules move down their concentration gradient diffusing out of OMBs to reach RBCs in the PM blood capillaries (Figure 4.1). To reach the capillaries in the peritoneum, oxygen must first dissolve in the saline of the OMBs and then diffuse through the mesothelium, cells and interstitial tissue. To reach the capillaries in the parenchymal tissue beneath the PM, oxygen must first dissolve in the saline of the OMBs and then diffuse through the PM layers and muscle tissue (Figure 4.2). The rate of diffusion depends on the surface area of the PM and the flux density. Increasing the area or the concentration gradient leads to faster diffusion. The diffusion rate using Fick's first law is written as

$$J = -AD \left(\frac{dC}{dx} \right)_{x=L} = -AD \frac{C_0 - C_s}{L} \tag{1}$$

where the diffusion zone is equal to the thickness (*L*) of the tissue between the OMBs and blood capillary wall, C_0 and C_s are the dissolved O_2 concentrations in blood capillaries and in the peritoneal cavity, respectively, *D* is the diffusivity, and *A* is the surface area of the PM, which can be calculated using the rat's mass (*M*) [44]

$$A(in\ cm^2) = 1.61M(in\ g) + 40.5 \tag{2}$$

The dissolved gas concentration at equilibrium depends on both partial pressure (P) and solubility (α) according to Henry's law

$$C = \alpha P \tag{3}$$

The parameters of solubility and diffusivity for O_2 in plasma and tissue are 0.003 (mL/dL)/mmHg and 1.7×10^{-5} cm^2/s, respectively [45]. The PM has a reported thickness of approximately 90 μm in rats [46]. However, because rats have relatively few blood vessels in the peritoneum, most oxygen transport could end in parenchymal tissue blood vessels, which are below the PM at a thickness between $0.5 - 1$ mm [47]. Both cases are examined in the calculation of the diffusion rate. If diffusion occurs over the PM by itself, O_2 will be absorbed by blood capillaries at peritoneum thickness of 90 μm (case 1). In contrast, if diffusion reaches the visceral organ capillaries, then the average tissue thickness is 0.75 mm (case 2). We used Fick's second law [48] that predicts how diffusion causes the concentration (C_x) to change with time. The solution to Fick's second law [48] is

$$\frac{C_x - C_0}{C_s - C_0} = 1 - erf\left(\frac{x}{2\sqrt{(Dt)}}\right) \tag{4}$$

where x is the thickness of tissue and t is time.

MATLAB was used to solve and plot C_x (Appendix D). In addition, the oxygen supply from OMBs was compared to the oxygen metabolism in resting rats, which is ~12 mL/min/kg [49].
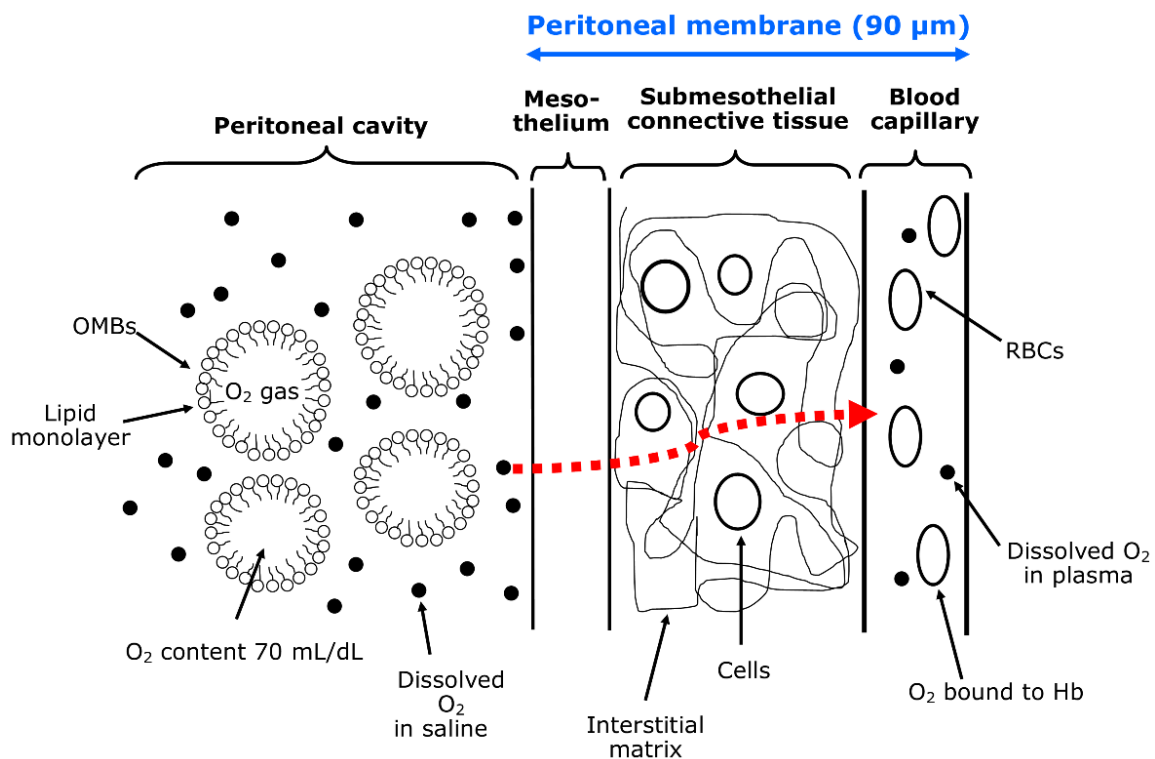
Figure 4.1 Simplified model of oxygen diffusion from OMBs to the layers of the

peritoneum
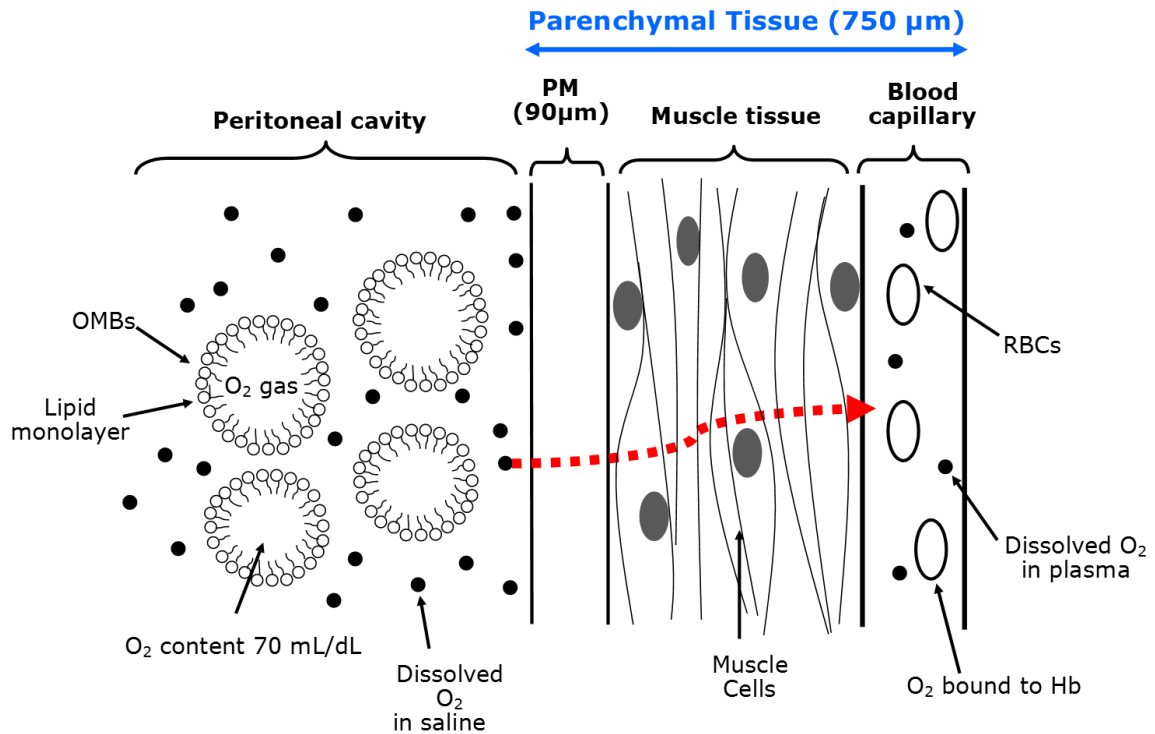
Figure 4.2 Simplified model of oxygen diffusion from OMBs to the layers of

parenchymal tissue

4.3 Results and Analysis

A simplified model for diffusion of oxygen from OMBs to the peritoneum blood was constructed. The mass of rats used in the mathematical model was 538 g, equal to the average mass of rats used in the *in vivo* experiments. Using equation 2, the peritoneal surface area was calculated to be 907 cm^2. The oxygen partial pressure (P_{O2}) in the peritoneal blood capillaries is normally 40 mmHg [50]. The average rat IP pressure measured after a single bolus injection of OMBs was ~2 mmHg above atmospheric pressure, so P_{O2} in OMBs was 762 mmHg. Thus, the pressure gradient of OMBs-to-blood was 722 mmHg.

The oxygen content inside OMBs is 70 mL/dL, while O_2 bound to hemoglobin in RBCs has a concentration of 15 mL/dL within venous blood. However, the diffusion rate is driven by the dissolved oxygen concentration gradient. Using equation 3, the concentration of dissolved O_2 in venous blood is C_0, which is equal to 0.12 mL/dL, while the concentration of dissolved O_2 in OMB saline is C_s, which is equal to 2.29 mL/dL. The OMBs-to-blood dissolved O_2 concentration gradient is their difference of 2.17 mL/dL.

An algorithm was developed using MATLAB to solve and plot the oxygen diffusion kinetics. If the diffusion thickness is 90 µm, then the oxygen diffusion rate would be 0.038 mL/s, and this supplies 34.4% of the total oxygen consumption needed in rats. However, if the thickness is 0.75 mm, then the diffusion rate would be 0.0045 mL/s supplying only 4.2% of the total oxygen consumption of rats. Tissue at depth of 90 µm (Figure 4.3a) will reach O_2 concentration of 1.94 mL/dL within 1 minute. Steady state is reached after 35 seconds. Tissue at depth of 0.75 mm (Figure 4.3b), will reach O_2 concentration of 1.77 mL/dL within 30 minutes. Steady state is reached after 41.7 minutes.

These results show that in theory oxygen delivered by OMBs *in vivo* occurs at a range between 0.0045 and 0.038 mL/s. Since oxygen delivery requires time (up to 42 min) to reach steady state, a bolus dosage administered periodically to IP cavity would be more efficient and cost effective than continuous infusion of OMBs. A 60 mL bolus would require a maximum dwell time of approximately 42 min to reach steady state in diffusion, but further *in vivo* tests are required to validate this dwell time.
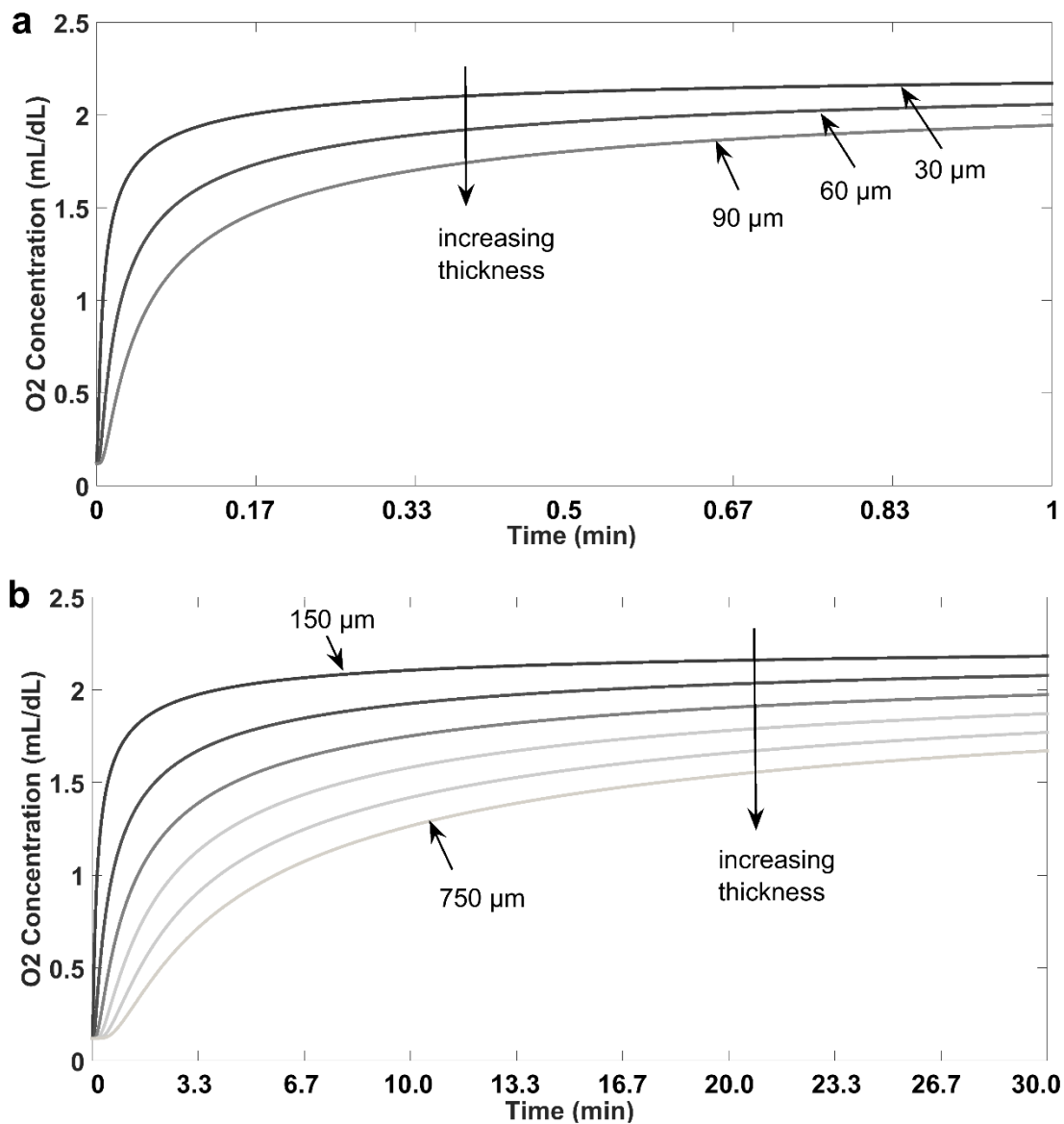
Figure 4.3 Mathematical model of 1D diffusion of oxygen from OMBs to peritoneal

blood over time

Chapter 5: *In vivo* Study

5.1 Introduction

In chapter 4, we have developed a simple model that predicts oxygen delivery from OMBs injected intraperitoneally. In theory the oxygen diffusion rate was found to be between 0.0045and 0.038 mL/s. This range for diffusion rate is relatively wide due to several modeling limitations including 1D pathway and no oxygen consumption by tissue considerations. To validate our model and to obtain a more precise oxygen transport rate, an *in vivo* experiment was designed. A previous study by Kheir et al. [35] showed that OMBs when mixed with deoxygenated blood *ex vivo* deliver O_2 in 4 sec. The purpose of this experiment is to study not only oxygen delivery by OMBs, but also possible CO_2 absorption and other gas(s) from surrounding tissue *in vivo*. To validate gas diffusion properties of OMBs *in vivo*, the gas content of OMBs was measured by a gas analyzer before and after injection to the rat's IP cavity. Fresh OMBs ideally contain pure oxygen gas if handled carefully avoiding air contamination. Measured gas concentrations were further converted to volumes and diffusion rate and depth were calculated. The experimental results for diffusion were then compared to the modeled theoretical values.

5.2 Materials and Methods

Male Wistar rats ($n = 4$, 538 ± 48 g) were housed and acclimated for four days, and cared for according to the University of Nebraska-Lincoln IACUC guidelines. All rats were sedated using ketamine-xylazine (18-2 mg/kg) and placed in the supine position

on a warming pad (T/pump Classic, Gaymar, Orchard Park, NY) set at 38 °C to maintain

body temperature (Figure 5.1a). Pulse oximetry (PhysioSuite, Kent Scientific Corp.,

Torrington, CT) measurements were taken throughout the whole experiment to measure

the heart rate (HR) and oxy-hemoglobin saturation (S_pO_2). The pulse oximeter clip was

placed on the rat's hind leg and data was recorded every second until the experiment was

terminated. After the rat was fully sedated and unresponsive to pain delivered by paw

pinches, a small incision into the skin was made to expose the fascia of the abdominal

wall. An inflow tube (3.2 mm, Tygon) and outflow catheter (JP7, Mila International Inc,

Erlanger, KY) were surgically implanted in the IP cavity and sutured closed (Figure

5.2b). A valve was placed on the exterior end of the outflow catheter to vacuum the line

with a syringe. A pressure sensor (S7d, Gaeltec Devices Ltd., Isle of Skye, UK) and the

injection syringe were connected to the inflow line. IP pressure was monitored and

maintained below 6 mmHg to avoid disruption of hemodynamics in the rat's abdomen

[51] [40]. The gas content of a 10 mL OMB sample collected directly from the OMB vial

was analyzed before injection ($t = 0$). A single 60 mL OMB bolus, a safe volume for

intraperitoneal injection of fluid in rats [38], was infused within 1 minute into the IP

cavity using the inflow line. Immediately after, the IP pressure was recorded.

Subsequently, 10 mL OMB samples were collected from the IP cavity every 5 minutes.

Samples were manually crushed in the syringe by applying pressure to the plunger and

then placed on a heating pad (70 °C) for 10 minutes (Figure 5.1b). This technique broke

the lipid monolayer of the OMBs and released the gas content of the sample into the

headspace (Figure 5.2c). The gas headspace was carefully transferred to another syringe

to be analyzed by an O_2 and CO_2 headspace gas analyzer (Gaspace 6600, Illinois Instruments, Inc., Johnsburg, IL). The syringe containing the gas sample was introduced into the gas analyzer by auto-injection (Figure 5.1c and Figure 5.2d). The entire process avoided air contamination to get the most reliable reading. Finally, after 20 minutes and 4 OMB samples were collected rats were euthanized by CO_2 inhalation.

One way valves were a source of inevitable air contamination added to each sample. The total volume of contamination, V_{air}, was found to be approximately 0.85 mL and composed of atmospheric air. A species balance was used to find the adjusted sample concentrations (x_{sample}) for O_2, CO_2 and N_2 neglecting water vapor and other trace gases. The overall volume balance was found with the following equations.

$$x_{O2,sample} = x_{O2,measured}\left(\frac{V_{air}}{V_{sample}} + 1\right) - 0.21\left(\frac{V_{air}}{V_{sample}}\right) \tag{5}$$

$$x_{N2,sample} = (1 - x_{O2,measured} - x_{CO2,measured})\left(\frac{V_{air}}{V_{sample}} + 1\right) - 0.79\left(\frac{V_{air}}{V_{sample}}\right) \tag{6}$$

$$x_{CO2,sample} = x_{CO2,measured}\left(\frac{V_{air}}{V_{sample}} + 1\right) \tag{7}$$

5.3 Statistical Analysis

A linear mixed model with repeated measures with AR(1) covariance structure followed by a t-test were performed on the estimated slopes and intercepts of recorded S_pO_2 data before injection and after injection of OMBs. A p-value threshold of 0.05 was considered statistically significant.
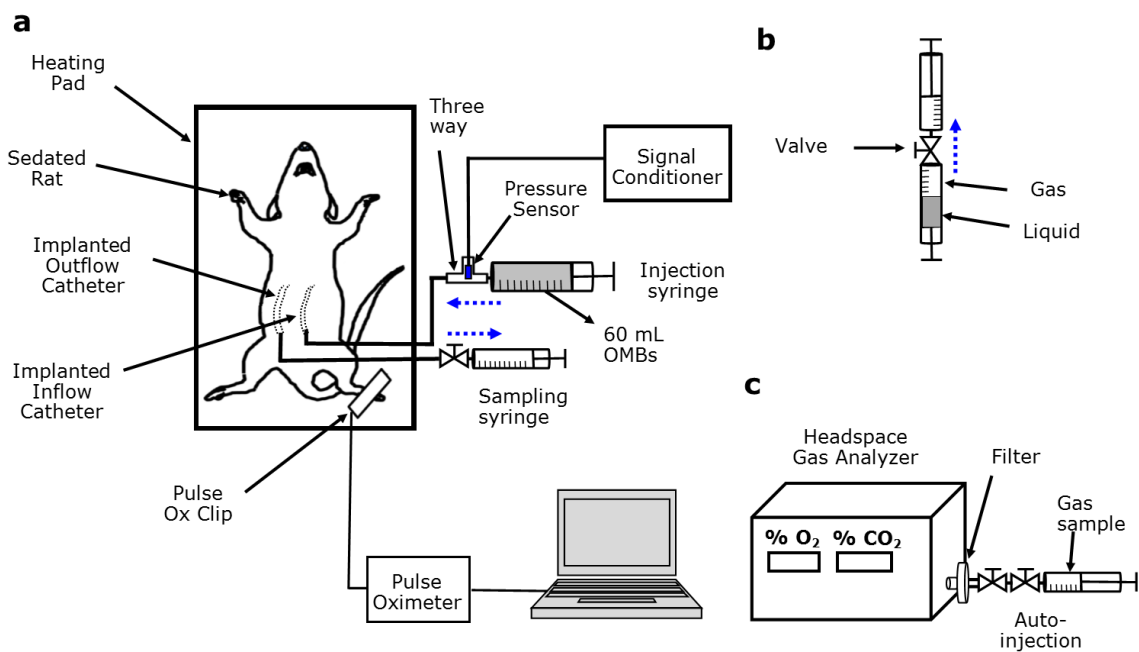
Figure 5.1 Experimental setup for headspace gas analysis of OMBs
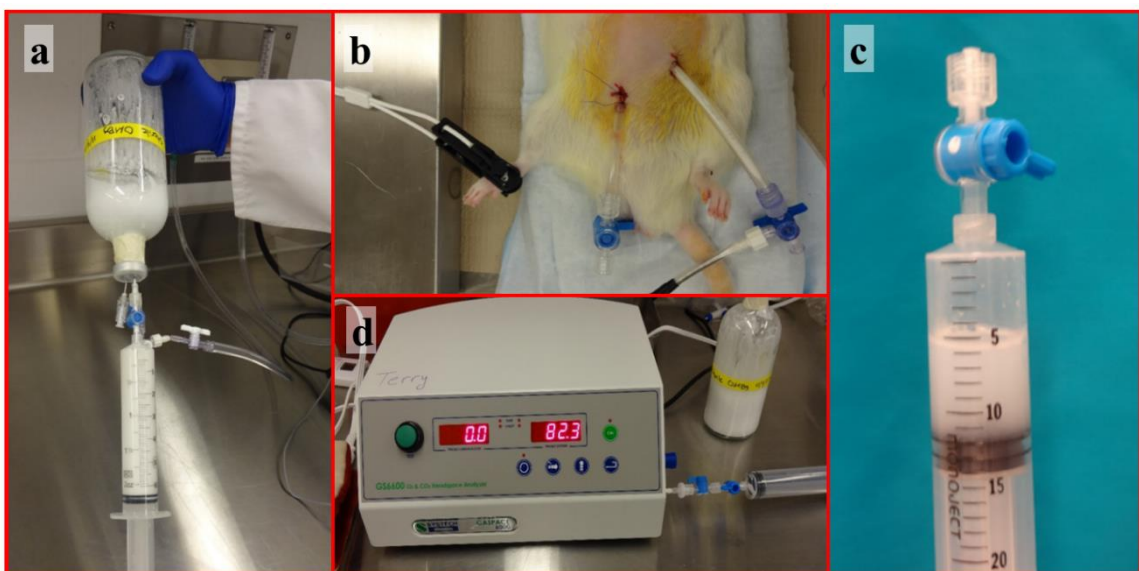
Figure 5.2 Pictures taken during experiment (a) OMB extraction (b) implanted catheters

(c) crushed OMBs (d) headspace gas analysis

5.4 Results and Analysis

Intraperitoneal pressure was recorded after OMB bolus injection. The average measurement was 1.93 ± 0.5 mmHg ($n = 4$). Before injection of OMBs at time 0 (Figure 5.3), the rats' average S_pO_2 was approximately $83.8 \pm 0.8\%$, while the average HR was 231.0 ± 10.3 bpm. After OMB bolus injection and 20 minutes dwell time, S_pO_2 increased to $86.2 \pm 2.2\%$, while HR decreased to 226.2 ± 9.0 bpm. The fitted linear regression model for S_pO_2 data showed that the slope of the line before injection was $- 0.0043$ indicating that there was no change in S_pO_2 and had no statistically significant increase with time ($p > 0.05$). After injection of OMBs, there was a slight increase of S_pO_2 after dwell with a slope of $+0.057$, which was found to be statistically significant ($p < 0.05$) using the same model and statistical test.

After crushing the OMBs, the gas volume was recorded for each sample (Figure 5.4a). Fresh OMBs had 67% gas volume fraction. This fraction decreased to $34.6 \pm 8.2\%$ after 20 minutes of dwell time. The measured gas contents were adjusted for contamination using equations 5, 6 and 7. Figure 5.4b shows the adjusted gas content detected in OMBs before and after dwelling in the IP cavity. Fresh OMBs had an average of $93.8 \pm 3.9\%$, 0% and $6.2 \pm 3.9\%$ for O_2, CO_2 and N_2, respectively. After 20 minutes of dwell time, OMBs had an average of $76.3 \pm 7.7\%$, $5.5 \pm 1.2\%$ and $17.2 \pm 7.6\%$ for O_2, CO_2 and N_2, respectively.
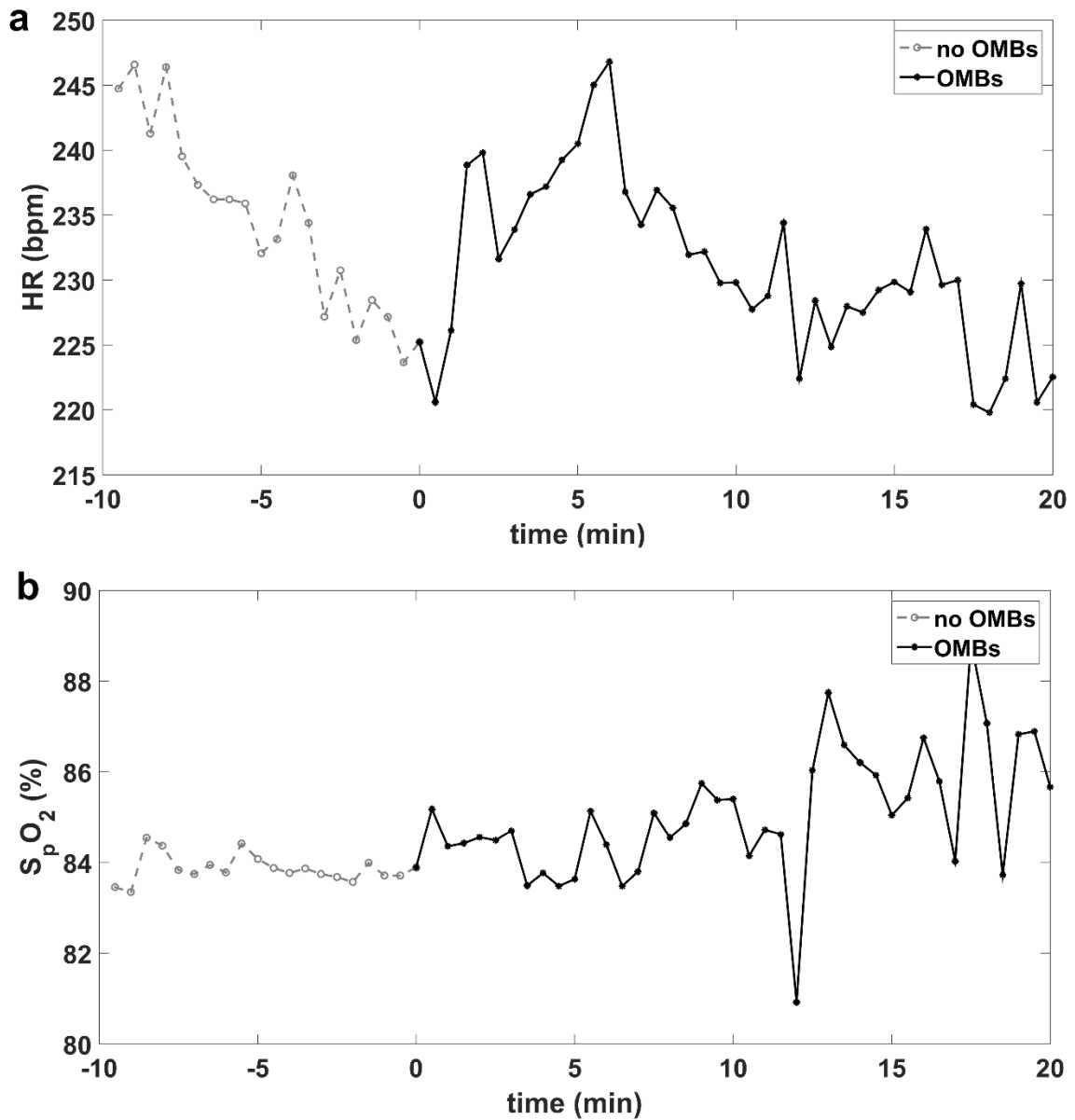
Figure 5.3 Pulse oximeter measurements (LS-mean) include (a) heart rate (beats per minute) and (b) oxy-hemoglobin saturation (%) before and after OMB bolus injection to the rat's IP cavity (n = 4)
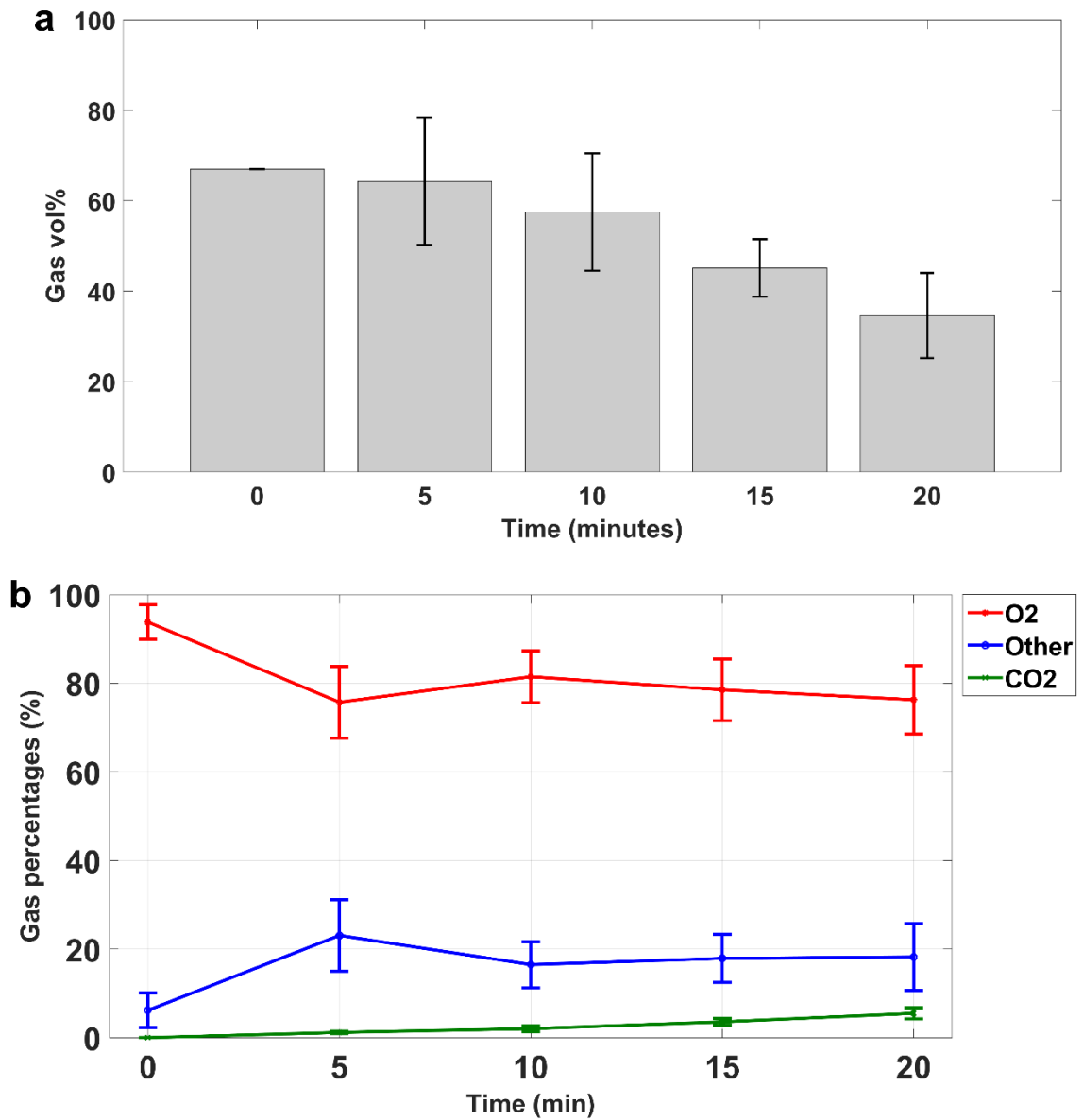
Figure 5.4 (a) Gas vol% composition (average ± SD) of OMBs and (b) gas content of

OMBs after OMB infusion to the cavity (n = 4)

Gas percentages obtained by the gas analyzer were further analyzed to determine the volume of O_2 that diffused from OMBs to the rat's body. The calculated diffusion volumes of O_2, CO_2 and N_2 across the PM over 20 min are shown in Table 5.1. Negative values represent diffusion in the opposite direction, from the rat's body into the OMBs. OMBs in the IP cavity had a total of 16.5 mL O_2 diffused over 20 minutes. This was equivalent to a diffusion rate of 0.014 mL/s. OMBs still carried 57.6 % of their initial O_2 volume after 20 min of dwell. Using the obtained diffusion rate, the diffusion depth was calculated to be 236 μm, and the oxygen supply was 13.1% of the total need. These values were within the range of our calculated theoretical diffusion model shown in Table 5.2.

These results indicate that after 20 minute dwell duration, OMBs (60 mL) still carry more than half of their initial oxygen content. In theory, a 45 min dwell would be enough time for oxygen to diffuse. These results confirm our bolus volume and dwell time predicted by our model in chapter 4. Therefore, for ~ 500 g rats a bolus volume of 60 mL OMBs will be allowed to dwell for ~ 45 minutes in the IP cavity of rats. Additional trials are needed to test this dwell duration on hypoxic rats.

Table 5.1 Diffused volume (average ± SD) of gases in mL between OMBs and

surrounding tissue during dwell in IP space (n = 4)

Time (min)	V_{OMBs} in IP	V_{O2} diffused	V_{CO2} diffused	V_{N2} diffused
0	60	--	--	--
5	60	9.8 ± 4.4	-0.4 ± 0.1	-5.2 ± 2.2
5+	50	--	--	--
10	50	-1.4 ± 5.5	-0.2 ± 0.2	2.3 ± 2.9
10+	40	--	--	--
15	40	4.4 ± 1.8	-0.2 ± 0.2	0.3 ± 0.9
15+	30	--	--	--
20	30	3.6 ± 1.8	-0.3 ± 0.2	0.3 ± 0.4

Table 5.2 Modeled versus experimental diffusion rate (J), diffusion depth (L) and oxygen

supply

	Model		Experiment
	Case 1	Case 2	
Depth (μm)	90	750	236
Rate (mL/s)	0.038	0.0045	0.014
% O_2 supply	34.4	4.2	13.1

Chapter 6: Discussion and Conclusions

Our first experiment determined a reliable and efficient method to extract the OMBs from the intraperitoneal space. A peritoneal lavage catheter (JP7, Mila International) can be used for long term studies involving OMB treatment of rats with mild to severe ARDS. This catheter can be surgically implanted in the IP space and used for both infusion and scavenging of OMBs due to its flexibility, wide diameter, numerous pores, and increased length. In addition, this catheter can be used in experiments that requires extraction of OMBs from the IP space to test for CO_2 absorption and O_2 delivery by OMBs.

Testing the effect of PMO as a potential therapy for ARDS requires at least 3 days of treatment. Thus, rats need to be conscious and able to move freely around their cage during this study. We have designed and developed an infusion system that automatically and intermittently infuses bolus dosage of OMBs to a rat's IP cavity. The system will be used for studying PMO with conscious rats of mild to severe ARDS. We have completed a pilot study ($n = 2$) to verify the benefits of PMO therapy utilizing a continuous infusion device. There appears to be short-term improvement in reduction of hypoxia using pulse oximeter measurements of S_pO_2. However, the preliminary trial revealed advanced tissue obstruction and growth in the catheter after four days. This was a major problem as it prevented further removal of fluid from the cavity. Therefore, the design was revised to implement a periodic bolus system that is simpler and effective. This would allow OMBs to dwell in the cavity for gas exchange to occur between OMBs and peritoneum blood. Benchtop testing of the final design of the bolus delivery system has been successfully

completed. Since the tubing restraint was not working properly, a new design of a rat tether will be developed and tested shortly. In future trials, rats will be infused with either a bolus of sterile oxygenated saline, inert gas microbubbles (IMBs) as controls or OMBs for PMO therapy with four rats from each group. Upon completion of the device, we will evaluate the effect of PMO therapy on survival, lung health, and oxygen saturation.

The significance of this study was to give a better understanding of how oxygen microbubbles exchange gas with peritoneal tissue when infused to the IP cavity. A model for diffusion predicted how fast oxygen will diffuse across the multiple layers of tissue in the surrounding abdomen and how that relate to the normal oxygen consumption need. In theory oxygen delivered by OMBs *in vivo* occurs at a range between 0.0045 and 0.038 mL/s. This would supply between 4.2% and 34.4% of the total oxygen consumption needed in resting healthy rats.

There are several limitations to this mathematical model. The O_2 consumption by tissue in surrounding abdominal wall and internal organs was not accounted for. Oxygen consumption by tissue would decrease the amount of oxygen absorbed by blood capillaries. Also, it was assumed that OMBs maintain pure oxygen concentration, which was not the case *in vivo* because other gases diffuse into the bubbles as shown in the headspace gas measurements. The mathematical model was based on time and one dimensional space because of the complicated model schemes required for the true dynamics of diffusion in the 3D abdomen.

The diffusion profile obtained from the *in vivo* study was compared to the modeled diffusion profile. The calculated diffusion zone (236 µm) was larger than the

thickness of the PM (90 μm), but less than the parenchymal tissue thickness (750 μm).

This indicates that oxygen diffused past the PM to reach underlying tissue in the

abdominal wall and internal organs, however oxygen did not diffuse to the entire depth of

parenchymal tissue in rats (0.5-1 mm thick). In addition, the oxygen supplied by the

OMBs (0.014 mL/s) was lower than the normal oxygen consumption of rats as expected

because the study was conducted on healthy rats. In addition to having catheter problems

using the continuous infusion system, these results changed our initial device design from

continuous circulation of OMBs to bolus periodic delivery. A 60 mL OMB bolus would

require a dwell time of approximately 45 min to reach steady state in gas exchange, but

further *in vivo* tests are required to validate this dwell duration on ARDS rats.

Pulse oximeter data indicated that bolus injection of OMBs did not cause any

harm to the animal's condition. General anesthesia causes low oxygen saturation and HR

measured by peripheral pulse oximetry [52]. After 20 min, there was a slight increase in

S_pO_2 by ~2.5%. This increase was statistically significant though it may not be clinically

relevant. These results indicate that peritoneal membrane oxygenation was not harmful

and may be potentially effective in delivering oxygen to hypoxic rats.

The greater decrease in oxygen content (Figure 5.4b) measured at 5 min

compared to the 10 min sample could be due to air contamination. The outflow line was

manually vacuumed directly after implantation into the IP cavity. Since this is not a

perfect vacuum and it is unlikely that oxygen was reentering the OMBs, residual air

within the line may explain why the sample taken at 10 min had more % O_2 than the 5

min sample. Another contributing factor could be that the gas volumes of the samples

was different. Fresh OMBs are composed of 70% O_2, 30% saline, and <1% lipids. After

OMBs dwell in the IP cavity, gas diffuses from OMBs to the body and vice versa thus

changing the ratio of gas to saline volume. More oxygen diffused from OMBs than other

gases being absorbed by the bubbles, so the gas percentage decreased gradually with

time.

One of the gases detected in OMBs was CO_2, which cannot be due to air

contamination because room air has only 0.003% CO_2 [53]. This gives evidence that

OMBs can uptake CO_2 from the body. Healthy rats have a low blood concentration of

CO_2, which explains the low amount of CO_2 detected in OMBs after dwelling in the IP

cavity. Other traces of gases are unknown but assumed to be N_2 because the nitrogen

partial pressure in venous blood is 573 mmHg [54]. Venous P_{N2} is much greater than

venous P_{CO2}, P_{O2}, and P_{H2O} which are 46, 40, and 47 mmHg, respectively. Fresh OMBs

have P_{O2} of 760 mmHg and P_{N2} of 0 mmHg ideally. Thus, there is a high blood-to-OMBs

nitrogen pressure gradient that leads to a flux of N_2 from surrounding venous tissue to

OMBs dwelling in the IP space. This may be of great potential benefit for removal of

excess nitrogen gas in decompression sickness, a common condition that affects divers

[55]. Further testing will be conducted to validate the other gas(s) absorbed by OMBs.

In conclusion, we developed a preliminary mathematical model that portrays the

kinetics of oxygen transfer between OMBs and the body. *In vivo* results show that

oxygen was delivered from OMBs by diffusive transport through the peritoneum into the

adjacent blood and tissue of the abdominal wall and internal organs. CO_2 was also able to

diffuse from the body into OMBs. Also, peritoneal oxygenation with OMBs did not

negatively alter the physical condition of the rats. Both mathematical modeling and animal experiments were applied on healthy rats with normal levels of oxygenation and respiratory rate. This serves as a reference for future studies involving hypoxia. We are able to demonstrate *in vivo* that OMBs not only can provide O_2 to the body, but also can absorb CO_2 and possibly other gases, such as N_2, from the body. This is very significant as it provides an alternative extrapulmonary technique of ventilation that can have significant implications in the future.

Our future goals involve improving our model using advanced numerical methods or finite elements analysis (FEA) that would be more accurate in simulating diffusion of multiple gases [56]. The transport of O_2, CO_2, and N_2 will also be modeled in hypoxic conditions. During hypoxemia, a lower oxygen concentration in blood increases the OMBs-to-blood oxygen concentration gradient thus increases the oxygen diffusion rate. In contrast, CO_2 accumulation in blood and tissue during hypoxia will drive CO_2 diffusion in the opposite direction thus OMBs will absorb a higher amount of CO_2.

Future work will include *in vivo* experiments on a hypoxic rat model of acute respiratory distress syndrome where we predict faster transport of oxygen and a more significant removal of carbon dioxide from the body due to the respiratory system being compromised. The oxygen delivery rate will be evaluated in supplying enough oxygen to accommodate the compromised lungs. In addition, arterial blood gases will be taken before and after infusion of OMBs to rat's IP cavity and tested for clinically significant increase in PaO_2.

We will further study the potential side effects of infusing OMBs to the intraperitoneal space by conducting autopsy and toxicology tests of abdominal organs. In addition, one way to determine the fate of OMBs *in vivo* would be to radioactively label the lipids to test their absorption or breakdown. In addition, radioactive labeling O_2 gas would be another way to detect the pathway of oxygen delivered by OMBs.

The Berlin criteria used for classifying ARDS may also be used as a selection criteria for patients requiring peritoneal membrane oxygenation. PaO_2/FiO_2 is an important determinant of low levels of oxygen in blood. Further literature review and research need to be conducted to find a suitable selection criteria for ARDS patients requiring PMO.

Patients with mild-to-moderate ARDS can be potentially treated with PMO either in tandem with current ventilation practices such as mechanical ventilation or by itself. Infusion of OMBs intraperitoneally would provide supplemental oxygenation to surrounding tissue in the abdomen and blood. Pulmonary ventilation supported by MV and supplemental extrapulmonary ventilation provided by PMO would supply enough oxygen that will hopefully prevent these patients to reach end stage ARDS. This would decrease the chance of these patients requiring ECMO, which has a high mortality rate. We foresee the implementation of peritoneal membrane oxygenation as a treatment and first response aid for respiratory distress in intensive care units and combat field settings in the future.

References

[1] M.A. Matthay, L.B. Ware, G.A. Zimmerman, The acute respiratory distress syndrome, J. Clin. Invest. 122 (2012) 2731–2740. doi:10.1172/JCI60331.

[2] C. Roussos, A. Koutsoukou, Respiratory failure, Eur. Respir. J. Suppl. 47 (2003) 3s–14s.

[3] G.D. Rubenfeld, E. Caldwell, E. Peabody, J. Weaver, D.P. Martin, M. Neff, et al., Incidence and Outcomes of Acute Lung Injury, N. Engl. J. Med. 353 (2005) 1685–1693. doi:10.1056/NEJMoa050333.

[4] S. Vasilyev, R.N. Schaap, J. Mortensen, Hospital survival rates of patients with acute respiratory failure in modern respiratory intensive care units : An international, multicenter, prospective survey, Chest. 107 (1995) 1083–1088. doi:10.1378/chest.107.4.1083.

[5] J. Hogan, P. Smith, D. Heath, P. Harris, The thickness of the alveolar capillary wall in the human lung at high and low altitude, Br. J. Dis. Chest. 80 (1986) 13–18.

[6] R.A. Rhoades, D.R. Bell, Medical Phisiology: Principles for Clinical Medicine, Lippincott Williams & Wilkins, 2012.

[7] The Acute Respiratory Distress Syndrome: Pathogenesis and Treatment, (n.d.). http://www.ncbi.nlm.nih.gov/pmc/articles/PMC3108259/ (accessed March 10, 2016).

[8] S. Han, R.K. Mallampalli, The acute respiratory distress syndrome: from mechanism to translation, J. Immunol. Baltim. Md 1950. 194 (2015) 855–860. doi:10.4049/jimmunol.1402513.

[9]   K.M. Sutin, P.L. Marino, P.L. Marino, The little ICU book of facts and formulas, Lippincott Williams & Wilkins, Philadelphia, 2008.

[10] M. Ragaller, T. Richter, Acute lung injury and acute respiratory distress syndrome, J. Emerg. Trauma Shock. 3 (2010) 43–51. doi:10.4103/0974-2700.58663.

[11] Stillwaterising, Chest X-ray PA, [object HTMLTableCellElement]. https://commons.wikimedia.org/wiki/File:Chest_Xray_PA_3-8-2010.png (accessed April 18, 2016).

[12] Case 3 answers - Mechanical Ventilation - Sub-internship in Critical Care Medicine - Medeck 620 - University of Washington School of Medicine, (n.d.). http://courses.washington.edu/med620/mechanicalventilation/case3answers.html (accessed March 7, 2016).

[13] G.F. Nieman, L.A. Gatto, J.H.T. Bates, N.M. Habashi, Mechanical Ventilation as a Therapeutic Tool to Reduce ARDS Incidence, Chest. 148 (2015) 1396–1404. doi:10.1378/chest.15-0990.

[14] J.A. Milberg, D.R. Davis, K.P. Steinberg, L.D. Hudson, Improved survival of patients with acute respiratory distress syndrome (ARDS): 1983-1993, JAMA. 273 (1995) 306–309.

[15] L. Gattinoni, E. Carlesso, T. Langer, Clinical review: Extracorporeal membrane oxygenation, Crit. Care Lond. Engl. 15 (2011) 243. doi:10.1186/cc10490.

[16] R.H. Bartlett, A.B. Gazzaniga, M.R. Jefferies, R.F. Huxtable, N.J. Haiduc, S.W. Fong, Extracorporeal membrane oxygenation (ECMO) cardiopulmonary support in infancy, Trans. - Am. Soc. Artif. Intern. Organs. 22 (1976) 80–93.

[17] E.S. Kim, C.J. Stolar, ECMO in the newborn, Am. J. Perinatol. 17 (2000) 345–356. doi:10.1055/s-2000-13449.

[18] L.-C. Chiu, F.-C. Tsai, H.-C. Hu, C.-H. Chang, C.-Y. Hung, C.-S. Lee, et al., Survival predictors in acute respiratory distress syndrome with extracorporeal membrane oxygenation, Ann. Thorac. Surg. 99 (2015) 243–250. doi:10.1016/j.athoracsur.2014.07.064.

[19] K. Lewandowski, Extracorporeal membrane oxygenation for severe acute respiratory failure, Crit. Care. 4 (2000) 156–168. doi:10.1186/cc689.

[20] V.M. Ranieri, G.D. Rubenfeld, B.T. Thompson, N.D. Ferguson, E. Caldwell, E. Fan, et al., Acute respiratory distress syndrome: the Berlin Definition, JAMA. 307 (2012) 2526–2533. doi:10.1001/jama.2012.5669.

[21] I. Singh, Absorption of Oxygen from the Peritoneal Cavity and the Stomach, Q. J. Exp. Physiol. 24 (1934) 45–54. doi:10.1113/expphysiol.1934.sp000624.

[22] M.A. Labato, Peritoneal dialysis in emergency and critical care medicine, Clin. Tech. Small Anim. Pract. 15 (2000) 126–135. doi:10.1053/svms.2000.16542.

[23] S.J. Davies, Peritoneal dialysis—current status and future challenges, Nat. Rev. Nephrol. 9 (2013) 399–408. doi:10.1038/nrneph.2013.100.

[24] Dialysis, (n.d.). http://www.renaldiseases.org/dialysis.html (accessed April 18, 2016).

[25] K. Pawlaczyk, M. Kuzlan, K. Wieczorowska-Tobis, H. Pawlik-Juzków, A. Breborowicz, J. Knapowski, et al., Species-dependent topography of the peritoneum, Adv. Perit. Dial. Conf. Perit. Dial. 12 (1996) 3–6.

[26] N. Ansari, Peritoneal Dialysis in Renal Replacement Therapy for Patients with Acute Kidney Injury, Int. J. Nephrol. 2011 (2011). doi:10.4061/2011/739794.

[27] A.K. Al-Hwiesh, Percutaneous peritoneal dialysis catheter insertion by a nephrologist: a new, simple, and safe technique, Perit. Dial. Int. J. Int. Soc. Perit. Dial. 34 (2014) 204–211. doi:10.3747/pdi.2012.00160.

[28] X.-H.W. J-Y Zhang, Effect of oxygenation of transperitoneal ventilation on the death time after asphyxiation in rabbits, Minerva Anestesiol. 76 (2010) 913–7.

[29] S.R. Carr, J.P. Cantor, A.S. Rao, T.V. Lakshman, J.E. Collins, J.S. Friedberg, Peritoneal perfusion with oxygenated perfluorocarbon augments systemic oxygenation, Chest. 130 (2006) 402–411. doi:10.1378/chest.130.2.402.

[30] N. Matsutani, B. Takase, Y. Nogami, Y. Ozeki, M. Ishihara, T. Maehara, The peritoneum as a novel oxygenation organ: revitalization of intraperitoneal oxygenation, Shock Augusta Ga. 30 (2008) 250–253. doi:10.1097/shk.0b013e318162be0a.

[31] N. Matsutani, B. Takase, Y. Nogami, Y. Ozeki, S. Kaneda, T. Maehara, et al., Efficacy of peritoneal oxygenation using a novel artificial oxygen carrier (TRM-645) in a rat respiratory insufficiency model, Surg. Today. 40 (2010) 451–455. doi:10.1007/s00595-009-4104-8.

[32] J.J. Kwan, M. Kaya, M.A. Borden, P.A. Dayton, Theranostic Oxygen Delivery Using Ultrasound and Microbubbles, Theranostics. 2 (2012) 1174–1184. doi:10.7150/thno.4410.

[33] M.A.B. James J Kwan, Microbubble Dissolution in a Multigas Environment, Langmuir ACS J. Surf. Colloids. 26 (2010) 6542–8. doi:10.1021/la904088p.

[34] J.A. Feshitan, N.D. Legband, M.A. Borden, B.S. Terry, Systemic oxygen delivery by peritoneal perfusion of oxygen microbubbles, Biomaterials. 35 (2014) 2600–2606. doi:10.1016/j.biomaterials.2013.12.070.

[35] J.N. Kheir, L.A. Scharp, M.A. Borden, E.J. Swanson, A. Loxley, J.H. Reese, et al., Oxygen Gas–Filled Microparticles Provide Intravenous Oxygen Delivery, Sci. Transl. Med. 4 (2012) 140ra88-140ra88. doi:10.1126/scitranslmed.3003679.

[36] N.D. Legband, J.A. Feshitan, M.A. Borden, B.S. Terry, Evaluation of peritoneal microbubble oxygenation therapy in a rabbit model of hypoxemia, IEEE Trans. Biomed. Eng. 62 (2015) 1376–1382. doi:10.1109/TBME.2015.2388611.

[37] J.J. Kwan, M.A. Borden, Lipid monolayer dilatational mechanics during microbubble gas exchange, Soft Matter. 8 (2012) 4756–4766. doi:10.1039/C2SM07437K.

[38] R.C. NAIRN, Fluid transfer from the peritoneal to the pleural cavities in rodents., Br. J. Exp. Pathol. 38 (1957) 62–6.

[39] N. Lameire, W. Van Biesen, M. Van Landschoot, T. Wang, O. Heimbürger, J. Bergström, et al., Experimental models in peritoneal dialysis: a European experience, Kidney Int. 54 (1998) 2194–2206. doi:10.1046/j.1523-1755.1998.00179.x.

[40] G. Sánchez-Etayo, X. Borrat, B. Escobar, A. Hessheimer, G. Rodriguez-Laiz, P. Taura, Effect of intra-abdominal pressure on hepatic microcirculation: implications

of the endothelin-1 receptor, J. Dig. Dis. 13 (2012) 478–485. doi:10.1111/j.1751-2980.2012.00613.x.

[41] I. Sukhotnik, J. Mogilner, L. Hayari, V. Brod, R. Shaoul, N. Slijper, et al., Effect of elevated intra-abdominal pressure and 100% oxygen on superior mesenteric artery blood flow and enterocyte turnover in a rat, Pediatr. Surg. Int. 24 (2008) 1347–1353. doi:10.1007/s00383-008-2262-1.

[42] Tethered Mouse and Rat Infusion System, SAI Infus. Technol. (n.d.). http://www.sai-infusion.com/pages/tethered-mouse-rat-infusion-system (accessed March 8, 2016).

[43] N. Legband, L. Hatoum, A. Thomas, B. Kreikemeier-Bower, D. Hostetler, K. Buesing, et al., Peritoneal Membrane Oxygenation Therapy for Rats with Acute Respiratory Distress Syndrome, Prog. (n.d.).

[44] E. Breton, P. Choquet, L. Bergua, M. Barthelmebs, B. Haraldsson, J.-J. Helwig, et al., In vivo peritoneal surface area measurement in rats by micro-computed tomography (microCT), Perit. Dial. Int. J. Int. Soc. Perit. Dial. 28 (2008) 188–194.

[45] P.A. Low, T.D. Lagerlund, P.G. McManis, Nerve Blood Flow and Oxygen Delivery in Normal, Diabetic, and Ischemic Neuropathy, in: Int. Rev. Neurobiol., Academic Press, Inc, 1989: p. 374.

[46] S. Duman, S. Sen, A.I. Günal, G. Asci, F. Akcicek, A. Basci, How can we standardize peritoneal thickness measurements in experimental studies in rats?, Perit. Dial. Int. J. Int. Soc. Perit. Dial. 21 Suppl 3 (2001) S338-341.

[47] M.F. Flessner, Microcirculation in Peritoneal Exchange, in: Microvasc. Res. Biol. Pathol., Elsevier Academic Press, 2006.

[48] F.C. Campbell, Elements of Metallurgy and Engineering Alloys, ASM International, 2008.

[49] C.M. Bishop, The maximum oxygen consumption and aerobic scope of birds and mammals: getting to the heart of the matter., Proc. R. Soc. B Biol. Sci. 266 (1999) 2275–2281.

[50] R.N. Pittman, Regulation of Tissue Oxygenation, Colloq. Ser. Integr. Syst. Physiol. Mol. Funct. 3 (2011) 1–100. doi:10.4199/C00029ED1V01Y201103ISP017.

[51] T.S. R Sümpelmann, Hemodynamic, acid base and blood volume changes during prolonged low pressure pneumoperitoneum in rabbits, Br. J. Anaesth. 96 (2006) 563–8. doi:10.1093/bja/ael045.

[52] J.L. Atlee, Complications in Anesthesia, Elsevier Health Sciences, 2007.

[53] B.K. Walsh, M.P. Czervinske, R.M. DiBlasi, Perinatal and Pediatric Respiratory Care, Elsevier Health Sciences, 2013.

[54] K.L. McCance, S.E. Huether, Pathophysiology: The Biologic Basis for Disease in Adults and Children, Elsevier Health Sciences, 2013.

[55] J. Hall, The Risks of Scuba Diving: A Focus on Decompression Illness, Hawaii J. Med. Public Health. 73 (2014) 13–16.

[56] A.O. Frank, C.J. Chuong, R.L. Johnson, A finite-element model of oxygen diffusion in the pulmonary capillaries, J. Appl. Physiol. Bethesda Md 1985. 82 (1997) 2036–2044.

Appendix A: Aspirated OMB Volumes

Table A.1 Recorded volumes of aspirated OMBs from IP space in rats (n = 5)

Rats	Volume of aspirated OMBs (mL)						
	18G	16G	14G	11G	10G	SOTT	PLC
1	0	0	0	1	0	1	30
2	4	19	8	18	11	16	37
3	0	23	1	0	6	11	33
4	1	0	0	43	0	3	20
5	4	35	0	0	0	7	30
Mean ± SD	1.8 ± 2.1	15.4 ± 15.2	1.8 ± 3.5	12.4 ± 18.7	3.4 ± 4.5	7.6 ± 6.1	30 ± 6.3

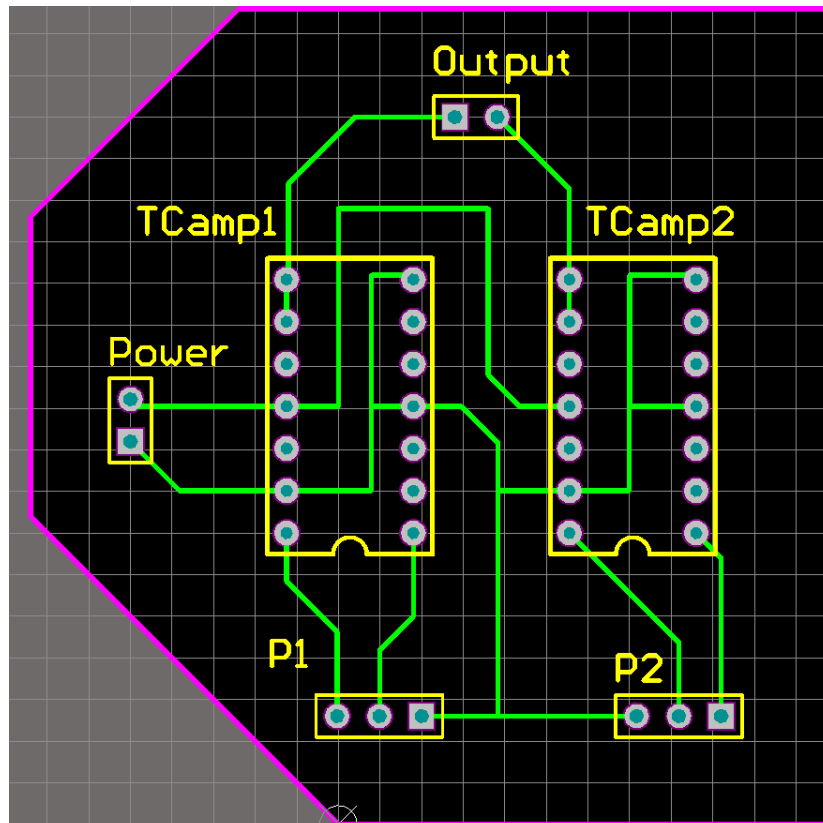# Appendix B: Temperature Circuit Design

Figure B.1 Temperature circuit board design using Altium

Appendix C: SolidWorks Drawings

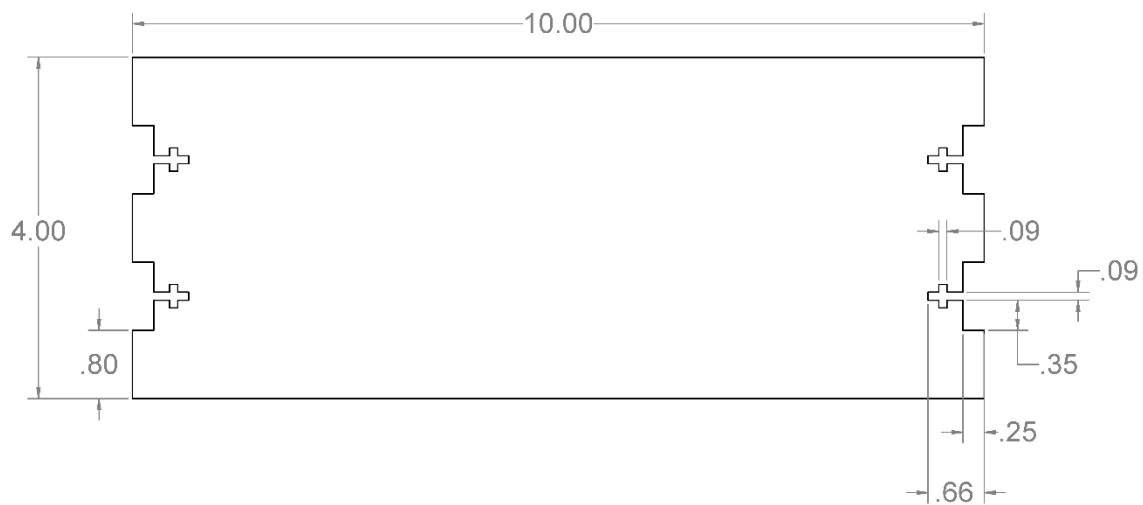Figure C.1 Lower face dimensions of electronics box

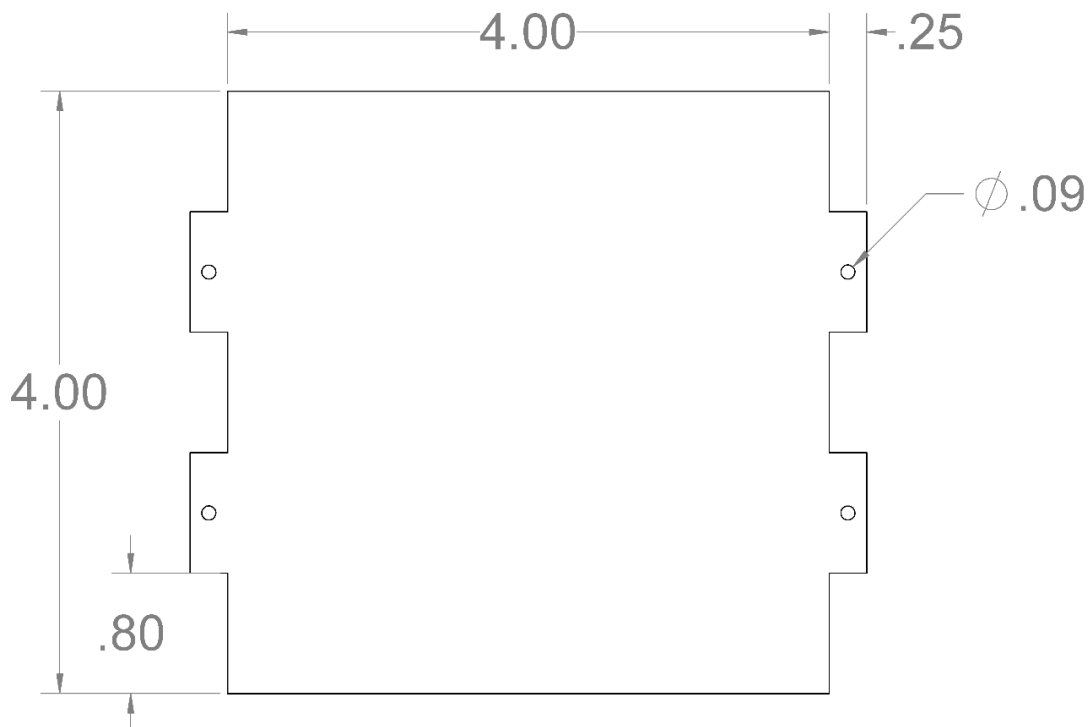Figure C.2 Top face dimensions of electronics box

Figure C.3 Side face dimensions of electronic box

Appendix D: Modeling Program

Matlab code for predicting the concentration change with time of peritoneum tissue after injection of OMBs.

```matlab
s = input('Please select case(1)/(2): ');
if s == 1
    x=0:.1:90;% thickness of PM (um)
    y=0:.1:60; %time (seconds)
else
    x=0:1:750;% thickness of parenchymal tissue(um)
    y=0:1:1800;
end

D = 1.7*10^3; %Diffusion coefficient of oxygen in tissue
(um2/s)
C0=0.12; % concentration of oxygen in plasma (ml/dl)
Cs=2.286; % concentration of oxygen in peritoneal cavity
filled with OMBs(ml/dl)

figure(2); hold on
n = length(x);

for i = 150:150:n
    X = x(i);
    K = ((C0-Cs)* erf(X./(2*sqrt(D.*y)))+Cs); %Solution to
Fick's second law where K is concentartion (ml/dl)
    plot(y,K,'LineWidth',3);
end
xlabel('Time (seconds)','Fontsize',24)
ylabel('O2 Concentration (mL/dL)','Fontsize',24)
```